DEUTSCHES ELEKTRONEN-SYNCHROTRON

DESY 93-084
July 1993

Inclusive Production of $K^*(892)$, $\rho^0(770)$, and $\omega(783)$ Mesons in the Υ Energy Region

The ARGUS Collaboration

ISSN 0418-9833

NOTKESTRASSE 85 - 22603 HAMBURG

To be sure that your preprints are promptly included in the
HIGH ENERGY PHYSICS INDEX,
send them to (if possible by air mail):

DESY **Bibliothek** **Notkestraße 85** **22603 Hamburg** **Germany**	**DESY-IfH** **Bibliothek** **Platanenallee 6** **15738 Zeuthen** **Germany**

DESY 93-084
July 1993
ISSN 0418-9833

Inclusive Production of $K^*(892)$, $\rho^0(770)$, and $\omega(783)$ Mesons in the Υ Energy Region

The ARGUS Collaboration

H. Albrecht, H. Ehrlichmann, T. Hamacher, R. P. Hofmann, T. Kirchhoff, A. Nau, S. Nowak[1], H. Schröder, H. D. Schulz, M. Walter[1], R. Wurth
DESY, Hamburg, Germany

C. Hast, H. Kapitza, H. Kolanoski, A. Kosche, A. Lange, A. Lindner, R. Mankel, M. Schieber, T. Siegmund, B. Spaan, H. Thurn, D. Töpfer, D. Wegener
Institut für Physik[2], Universität Dortmund, Germany

M. Bittner, P. Eckstein
Institut für Kern- und Teilchenphysik[3], Technische Universität Dresden, Germany

M. Paulini, K. Reim, H. Wegener
Physikalisches Institut[4], Universität Erlangen-Nürnberg, Germany

R. Eckmann, R. Mundt, T. Oest, R. Reiner, W. Schmidt-Parzefall
II. Institut für Experimentalphysik, Universität Hamburg, Germany

J. Stiewe, S. Werner
Institut für Hochenergiephysik[5], Universität Heidelberg, Germany

K. Ehret, W. Hofmann, A. Hüpper, S. Khan, K. T. Knöpfle, M. Seeger, J. Spengler
Max-Planck-Institut für Kernphysik, Heidelberg, Germany

D. I. Britton[6], C. E. K. Charlesworth[7], K. W. Edwards[8], E. R. F. Hyatt[6], P. Krieger[7], D. B. MacFarlane[6], P. M. Patel[6], J. D. Prentice[7], P. R. B. Saull[6], K. Tzamariudaki[6], R. G. Van de Water[7], T.-S. Yoon[7]
Institute of Particle Physics[9], Canada

D. Reßing, M. Schmidtler, M. Schneider, K. R. Schubert, K. Strahl, R. Waldi, S. Weseler
Institut für Experimentelle Kernphysik[10], Universität Karlsruhe, Germany

G. Kernel, P. Križan, E. Križnič, T. Podobnik, T. Živko
Institut J. Stefan and Oddelek za fiziko[11], Univerza v Ljubljani, Ljubljana, Slovenia

V. Balagura, I. Belyaev, S. Chechelnitsky, M. Danilov, A. Droutskoy, Yu. Gershtein, A. Golutvin, I. Korolko, G. Kostina, D. Litvintsev, V. Lubimov, P. Pakhlov, S. Semenov, A. Snizhko, V. Soloshenko, I. Tichomirov, Yu. Zaitsev
Institute of Theoretical and Experimental Physics, Moscow, Russia

[1] DESY, IfH Zeuthen

[2] Supported by the German Bundesministerium für Forschung und Technologie, under contract number 054DO51P.
[3] Supported by the German Bundesministerium für Forschung und Technologie, under contract number 055DD11P.
[4] Supported by the German Bundesministerium für Forschung und Technologie, under contract number 054ER12P.
[5] Supported by the German Bundesministerium für Forschung und Technologie, under contract number 055HD21P.
[6] McGill University, Montreal, Quebec, Canada.
[7] University of Toronto, Toronto, Ontario, Canada.
[8] Carleton University, Ottawa, Ontario, Canada.
[9] Supported by the Natural Sciences and Engineering Research Council, Canada.
[10] Supported by the German Bundesministerium für Forschung und Technologie, under contract number 055KA11P.
[11] Supported by the Department of Science and Technology of the Republic of Slovenia and the Internationales Büro KfA, Jülich.

Abstract

The production of $K^{*+}(892)$, $K^{*0}(892)$, $\rho^0(770)$ and $\omega(783)$ vector mesons in $q\bar{q}$ events as well as in the gluonic $\Upsilon(1S)$ decays and $\Upsilon(4S) \to B\overline{B}$ decays has been studied using the ARGUS detector. Combining these results with data on pseudoscalar meson, ϕ meson and baryon production collected with the same detector allow comprehensive studies of quark and gluon fragmentation. Model independent information on s quark and vector meson suppression ($s/u = 0.37 \pm 0.04$, $V/(V+P)_\pi = 0.21 \pm 0.04$ and $V/(V+P)_K = 0.34 \pm 0.03$)) are derived. The data are compared with predictions from the models Jetset 7.3 and UCLA 7.31.

1 Introduction

The study of e^+e^- annihilation in a wide range from DORIS II to LEP energies has been important to establish QCD as the theory of strong interaction [1]. The observation of gluons as quark bremsstrahlung and in $\Upsilon(1S)$ decays was a major breakthrough for the standard model [2]. More recently even direct evidence for the gluon selfcoupling as the manifestation of the nonabelian symmetry of the theory was observed at LEP [3].
In contrast to these processes with large momentum transfers the region of soft QCD is up to now not calculable from first principles. Therefore the formation of hadrons out of quarks and gluons has been carefully studied in many experiments to develop at least phenomenological models. However even with large data samples one can hardly disentangle correlated model parameters, so that the determination of properties of fragmentation remains difficult. All experiments on QCD suffer to a certain extent from this fact, as they need fragmentation models to predict the observable final states. It is therefore of great importance to compare precise data with models to check their predictive power and fix free parameters. Moreover basic properties of soft processes such as the relative production of states differing in their flavour and spin composition may serve as guidelines for future less model dependent approaches to describe fragmentation into hadronic final states.
The high statistics data samples collected with the ARGUS detector in the energy region of the Υ mesons are perfectly suited for studies on fragmentation. Stable hadrons can be identified, hence the reconstruction of resonances is possible with relative low background. The inclusive production of vector mesons in gluon fragmentation is studied in the decays $\Upsilon(1S) \to 3g$ and $\Upsilon(1S) \to 2g\gamma$, since in these events the charm content is small [4] and uncertainties on decays of charmed hadrons do not influence the interpretation. The continuum data can be used to test whether the fragmentation of quarks can be described by models with parameters fixed to reproduce gluonic $\Upsilon(1S)$ decays.
The paper is organized as follows: First, we describe the analysis of $K^{*+}(892)$, $K^{*0}(892)$, $\rho^0(770)$ and $\omega(783)$ production[1] in the gluonic $\Upsilon(1S)$ decays, $q\bar{q}$ events and $\Upsilon(4S)$ decays. The inclusive multiplicities and energy spectra are summarized and discussed in the second part.

[1] Unless otherwise stated references in this paper to a specific charged state are to be interpreted as implying the charge conjugate state as well.

2 Data samples and event selection

The data used in this analysis were collected with the ARGUS detector at the DORIS II storage ring at DESY. The data sample corresponds to an integrated luminosity of $26.7\,\mathrm{pb}^{-1}$ on the $\Upsilon(1S)$ resonance at the center of mass energies $\sqrt{s}$ =9.46 GeV, $213.4\,\mathrm{pb}^{-1}$ on the $\Upsilon(4S)$ at 10.58 GeV and $92.5\,\mathrm{pb}^{-1}$ in the nearby continuum. Beside these, $31.6\,\mathrm{pb}^{-1}$ on the $\Upsilon(2S)$ at 10.02 GeV have been used to study systematic effects in this analysis [5].
The ARGUS detector is a magnetic 4π spectrometer described in detail elsewhere [6]. The momenta of charged particles and their mean energy loss were measured with the drift chamber. Particles were identified using both specific ionization and time of flight measurements. The energy of photons was measured in the electromagnetic calorimeter. Reconstruction of decay vertices from neutral particles (i.e. K^0_S) was improved by a vertex drift chamber.

Hadronic events were selected by requiring at least three charged tracks from a reconstructed main vertex or three charged tracks, which do not necessarily point to a common vertex, but in addition at least an energy of 1.7 GeV deposited in the electromagnetic calorimeter. Two photon events, beam gas and beam wall interactions were suppressed by comparing the scalar momentum sum of all neutral and charged particles $P_{sum} = \frac{1}{\sqrt{s}} \cdot \sum |\vec{p}_i c|$ with the momentum sum along the beam direction $P_{sum,z} = \frac{1}{\sqrt{s}} \cdot \sum p_{i,z} c$ and demanding $P_{sum} > 0.315 + 2.5 \cdot P^2_{sum,z}$. Remaining radiative QED processes, where the photon converts into an e^+e^- pair, are rejected by requiring at least two detected photons in the calorimeter with an energy of more than 80 MeV.
The contribution of two photon events, beam gas and beam wall interactions and radiative QED reactions in the final event sample was estimated by comparing data and simulations to be less than 2% after these cuts. Hadronic τ decays from $e^+e^- \to \tau^+\tau^-$ cannot be suppressed totally by an event selection as long as a high efficiency for the studied events is demanded. Their contribution in the continuum event sample is estimated by a Monte Carlo simulation using the branching ratios from [7] to be 4% and less than 0.3% in Υ decays [5]. The τ contribution was subtracted when determining the total hadronic cross sections.

3 Determination of total hadronic cross sections

The total hadronic cross section (σ_{tot}) at $\sqrt{s}$ equal to the $\Upsilon(1S)$ mass is composed of continuum reactions ($\sigma_{q\bar{q}}$), of hadronic decays of τ leptons produced in e^+e^- annihilation and $\Upsilon(1S)$ decays ($\sigma_{\tau\tau,cont}$, $\sigma_{\tau\tau,res}$), and of hadronic $\Upsilon(1S)$ decays. The latter consist of direct decays into three gluons or two gluons and one photon (σ_{dir}) plus the vacuum polarization (σ_{vacpol}), where the resonance decays via a virtual photon.

$$\sigma_{tot} = \sigma_{q\bar{q}} + \sigma_{\tau\tau,cont} + \sigma_{dir} + \sigma_{vacpol} + \sigma_{\tau\tau,res}$$

With the relation

$$R = \sigma_{vacpol}/\sigma_{\tau\tau,res} = \sigma_{q\bar{q}}/\sigma_{\tau\tau,cont} \cdot 0.93$$

(the factor 0.93 takes into account the different contributions of initial state radiation) and the efficiencies η defined in table 1 the total visible hadronic cross section is a sum of five components:

$$\sigma^{vis}_{tot} = \sigma_{q\bar{q}} \cdot \left(\eta_{q\bar{q}} + 0.93 \cdot \frac{\eta_{\tau\tau}}{R}\right) + \sigma_{dir} \cdot \eta_{dir} + \sigma_{vacpol} \cdot \left(\eta_{vacpol} + \frac{\eta_{\tau\tau}}{R}\right).$$

Using lepton universality the total cross section of the resonance, σ_{tot}, can be written as

$$\sigma_{tot} = \sigma_{dir} + \sigma_{vacpol} + 3 \cdot \sigma_{\tau\tau,res} \quad .$$

With $B_{\mu\mu} = BR(\Upsilon(1S) \to \mu^+\mu^-) = \sigma_{\tau\tau,res}/\sigma_{tot}$ (lepton universality was used) one obtains

$$\sigma_{vacpol} = \sigma_{dir} \cdot \frac{R \cdot B_{\mu\mu}}{1 - B_{\mu\mu}(R+3)}$$

and finally achieves for the direct hadronic cross section:

$$\sigma_{dir} = \frac{\sigma^{vis}_{tot} - \sigma_{q\bar{q}} \cdot (\eta_{q\bar{q}} + 0.93 \cdot \eta_{\tau\tau}/R)}{\eta_{dir} + \frac{RB_{\mu\mu}}{1-B_{\mu\mu}(R+3)} \cdot (\eta_{vacpol} + \eta_{\tau\tau}/R)}.$$

The continuum below the resonance at an center of mass energy $\sqrt{s_{on}}$ must be extrapolated from the measurements off the resonance at $\sqrt{s_{off}}$. With the radiative corrections $\delta(s)$ (including QED and QCD effects), where $\sigma_{q\bar{q}}(s) = \sigma^0_{q\bar{q}} \cdot \delta(s)$, one obtains

$$\sigma_{q\bar{q}}(s_{on}) = \sigma_{q\bar{q}}(s_{off}) \cdot \frac{s_{off}}{s_{on}} \cdot \frac{\delta(s_{on})}{\delta(s_{off})} \quad .$$

The same calculation was used to determine the cross sections at the $\Upsilon(4S)$ and $\Upsilon(2S)$ resonances.
The selection efficiencies for various event types were determined with the help of Monte Carlo calculations including a detailed simulation of the ARGUS detector. The Lund 6.3 model [8] was used to simulate continuum events and Υ decays. The efficiencies were parametrized as functions of the number of charged tracks, which could be reconstructed after detector simulation, and the acceptance correction was performed on an event by event basis. Averaged efficiencies for different event types can be found in table 1. To combine continuum data at

Event type	Efficiency	
$e^+e^- \to q\bar{q}$	η_{vacpol}	$= (87.9 \pm 0.2)\%$
$e^+e^- \to q\bar{q}(\gamma)$	$\eta_{q\bar{q}}$	$= (80.5 \pm 0.2)\%$
$\Upsilon(1S)$-dir	η_{dir}	$= (94.2 \pm 0.1)\%$
$\Upsilon(4S) \to B\overline{B}$	$\eta_{\Upsilon(4S)}$	$= (95.6 \pm 0.1)\%$
$e^+e^- \to \tau^+\tau^-$	$\eta_{\tau\tau}$	$= (10.7 \pm 0.2)\%$

Table 1: The efficiency of the ARGUS trigger followed by the event selection for continuum events including initial state bremsstrahlung of photons, for Υ decays and τ events. The errors include statistical uncertainties only.

different energies one has to take into account radiative corrections depending on $\sqrt{s}$. This was done by using the event generator Lund 6.3 with implemented quarkonia resonances that can be directly produced via a virtual photon [5]. Continuum results are referred to $\sqrt{s}$ = 10.45 GeV in the following sections.
Systematic uncertainties for the total cross sections stem from time variations in the detector performance, accuracy of the luminosity measurement and differences between simulations and data. Additional contribution for the resonance decays originate in the scaling of the continuum data to the $\Upsilon(1S)$ energy and in the precision of $B_{\mu\mu}$. Using $B_{\mu\mu} = (2.57 \pm 0.07)\%$ [7] the final results are given in table 2. Here $\sigma^0_{q\bar{q}}$ denotes the continuum cross section in the lowest order of QED.

Event type	cross section [nb]
Cont. (10.45 GeV)	$\sigma_{q\bar{q}} = 3.60 \pm 0.11$
Cont.,rad.cor. (10.45 GeV)	$\sigma^0_{q\bar{q}} = 2.86 \pm 0.09$
$\Upsilon(1S)$ direct	$\sigma_{dir} = 8.24 \pm 0.26$
$\Upsilon(4S) \to B\overline{B}$	$\sigma_{\Upsilon(4S)} = 0.88 \pm 0.07$

Table 2: Measured cross sections for different event types. The continuum result is given as measured and in the lowest order of QED (radiation corrected).

4 Determination of inclusive meson spectra and multiplicities

The inclusive particle production cross sections are determined as functions of the scaled meson energy

$$z = \frac{2 \cdot E_{meson}}{\sqrt{s}} .$$

The spectra are weighted with $1/\beta$, where β denotes the particle's velocity in units of c, and normalized to the measured total hadronic cross section σ_{had} of the analysed event type. Hence the presented spectra can directly be compared to other results at different center of mass energies and to Monte Carlo calculations, which predict a number of mesons n generated in N_{had} events.

$$\frac{1}{\beta\sigma_{had}} \cdot \frac{d\sigma}{dz} = \frac{1}{\beta N_{had}} \cdot \frac{dn}{dz}$$

The differential continuum cross sections were corrected for initial state radiation of photons and scaled to the resonance energies to subtract them from the data at these energies with a method similar to the one used for the total hadronic cross section, but considering also the variation of the z spectra. For all vector mesons the radiation corrections lead to an increase of dn/dz between approximately 8% at z=0.2 and 14% at z=0.9. This correction method was tested by comparing the measured spectra of K^{*0} mesons at the c.m.s energies of 9.36 and 10.45 GeV. The observed relation between the two data sets agrees with the scaling procedure applied [5]. To derive the particle spectra from direct $\Upsilon(1S)$ decays the contributions of continuum and the vacuum polarization have to be subtracted. As the final state of the vacuum polarization corresponds to continuum events without initial state radiation of photons the radiatively corrected spectra measured for continuum events multiplied with $\sigma_{vacpol}/\sigma^0_{q\bar{q}}$ and scaled to the $\Upsilon(1S)$ mass were used to estimate the contributions from $\Upsilon(1S)$ decays via a virtual photon. An example of the different contributions in the $\Upsilon(1S)$ data is shown in figure 1.
The contaminations from τ decays have not been subtracted, as they are always smaller than the systematic uncertainties. Using the branching ratios given in [7] the remaining meson multiplicities from τ decays are shown in table 3 for continuum data.

Meson	n_τ(meson)
K^{*+}	0.0019 ± 0.0003
K^{*0}	0.0011 ± 0.0003
ρ^0	0.017 ± 0.005
ω	0.012 ± 0.004

Table 3: Vector meson multiplicities from $e^+e^- \to \tau^+\tau^-$ and subsequent hadronic τ decays per continuum event contained in the inclusive continuum multiplicities (compare table 7).

4.1 Reconstruction of vector mesons

The vector mesons were reconstructed by analysing the invariant mass spectra of their decay products. Table 4 shows the decay channels with the corresponding branching ratios used in this analysis. To reconstruct these vector mesons it was necessary to detect charged and neutral particles as well as decay vertices of K^0_S mesons. To select particles with high efficiencies a minimum momentum of 200 MeV/c for charged pions and 300 MeV/c for kaons was demanded. The momentum transverse to the beam axis had to exceed 60 MeV/c and the angle θ of the particle's direction of flight with respect to the beam axis had to fulfill $|\cos\theta| < 0.92$. Pions originating from K^0_S or K^{*+} decays had to have a momentum larger than 100 MeV/c. All charged particles had to point to the main vertex or point to a secondary K^0_S vertex with a χ^2 of less than 36. They were accepted as pion or kaon candidates, if the corresponding normalized likelihood calculated from the dE/dx and ToF measurements exceeded 0.1.

Decay mode	BR
$K^{*+} \to K^0\pi^+$ with $K^0 \to K^0_S \to \pi^+\pi^-$	$(22.9 \pm 0.1)\%$
$K^{*0} \to K^+\pi^-$	$(66.7 \pm 0.2)\%$
$\rho^0 \to \pi^+\pi^-$	$(99.9 \pm 0.1)\%$
$\omega \to \pi^+\pi^-\pi^0$ with $\pi^0 \to \gamma\gamma$	$(88.8 \pm 0.6)\%$

Table 4: The vector meson decay channels used with their branching ratios [7].

The decay vertices of K^0_S mesons were required to have a distance from the beam line between 1.5 cm and 25 cm. The reconstructed K^0_S momentum had to point to the main vertex with $\chi^2 < 36$, the angle with the beam axis had to fulfill $|\cos\theta| < 0.8$. To suppress photons which converted into an e^+e^--pair in the detector material and to simplify the determination of the K^0_S efficiency a cut on the opening angle α between the two pions was applied: $-0.5 < \cos\alpha < 0.996$. Secondary vertices were accepted as K^0_S candidates if the invariant $\pi^+\pi^-$ mass is within 15 MeV/c^2 around the nominal mass and if the corresponding χ^2 of the mass measurement was less than two standard deviations. After this a mass constraint fit to the K^0_S mass was performed.
Photon candidates were accepted if their energy was not below 80 MeV and the angle θ fulfilled $|\cos\theta| < 0.92$. To reconstruct π^0 mesons two photons were combined and accepted as

candidates if their mass was consistent with the π^0 mass within $100\,\mathrm{MeV/c^2}$ and a corresponding χ^2 of less than 4. For these π^0 candidates a mass constraint fit was performed, too.

4.2 The Efficiency

To determine the efficiency, events were simulated according to the fragmentation model Lund 6.3 and afterwards passed through a detailed simulation of the ARGUS detector. These Monte Carlo events were processed and analysed in the same way as real data.
The efficiencies were factorized into a model dependent and a detector sensitive contribution [5]. The model dependent efficiency is only a function of the kinematical cuts on momenta and angles used in this analysis (see previous section). Typical examples of these efficiencies are shown in figure 2. The efficiencies for vector mesons fulfilling the kinematical cuts were determined as a product of the efficiencies of particles that can be observed in the detector. This factorization was not possible for the efficiency of ω mesons as the reconstruction probability of photons in the electromagnetic calorimeter depends on the overall characteristics of the events.
In figure 3 the total efficiencies to reconstruct vector mesons in continuum events are given as a function of their momenta. The low acceptance of ω mesons at high momenta is related to the reconstruction of π^0 mesons out of two photons. If the momentum of neutral pions exceeds $1\,\mathrm{GeV/c}$ the energy depositions of the decay photons in the calorimeter tend to overlap and the probability to identify two photons decreases. In general the efficiencies in continuum events are slightly lower than in direct $\Upsilon(1S)$ decays because of different angular distributions with respect to the beamline.
The efficiency corrections were performed by weighting every entry in the analysed histograms with the inverse efficiency.

4.3 The K^{*+} analysis

The energy spectra of the vector mesons were obtained by analysing the invariant mass distributions of their decay products in intervals of the scaled energy z. The observable mass spectra of the resonances result from the underlying real distributions convoluted with the resolution function of the detector. The mass resolutions range from 20 MeV for ω to 5.4 MeV for K^{*0} mesons. Due to the measurement of photon energies in the calorimeter the mass resolution for ω mesons is much broader than for K^{*0} mesons, which are reconstructed from two charged tracks. To derive the total multiplicities an extrapolation of the measured z spectra into the unobserved low momentum regions was performed. Details of the analyses are given in the following sections.
The K^{*+} signal is described by a relativistic Breit-Wigner function with an angular momentum L=1 [9]:

$$\mathrm{BW(m)} = \frac{\mathrm{m}\cdot\mathrm{m_0}\cdot\Gamma(\mathrm{m})}{(\mathrm{m_0^2}-\mathrm{m^2})^2+(\mathrm{m_0}\cdot\Gamma(\mathrm{m}))^2}$$

$$\Gamma(\mathrm{m}) = \Gamma_0\cdot\left(\frac{\mathrm{q}}{\mathrm{q_0}}\right)^{2\mathrm{L}+1}\cdot\frac{2\mathrm{q_0^2}}{\mathrm{q_0^2}+\mathrm{q^2}}$$

m_0	:	mass of resonance
Γ_0	:	width of resonance
L	:	angular momentum of decay products
q_0, q	:	momentum of decay products in the resonance c.m. system with masses m_0, m

Monte Carlo studies show that a convolution of this function with the resolution is not necessary, as the natural width dominates over the detector resolution. Detector effects can be entirely absorbed by increasing the width from the PDG value [7] of $\Gamma_0 = 50\,\mathrm{MeV/c^2}$ to $57\,\mathrm{MeV/c^2}$. As details of the signal's tail to high masses for mesons produced in fragmentation are yet unknown we determined the number of K^{*+} mesons by integrating the signal in a range of $\pm 2.5\cdot\Gamma_0$ around the nominal mass ($749 - 1035\,\mathrm{MeV/c^2}$).
Note that the Lund model uses nonrelativistic Breit-Wigner functions to simulate the decay of vector mesons. This difference between data and simulation was taken into account in the analysis.
With the selection criteria described above K_S^0-candidates from secondary vertices were combined with pion candidates from the main vertex. The background below the K^{*+}-signal shows a smooth behaviour without any reflections. This is confirmed by Monte Carlo studies. Therefore the whole mass spectrum was fitted in the range 0.65-1.2 $\mathrm{GeV/c^2}$ with the signal plus a polynomial times threshold factor to describe the background [5]. In spite of their different shapes the mass distributions from continuum, $\Upsilon(1S)$ and $\Upsilon(4S)$ data could be fitted with the same function, so that possible small discrepancies between data and simulations could be taken into account in the fitting procedure. This is the case also for the other analyses described in the following sections.
One example for the resulting mass spectra is shown in figure 4. Every entry has been weighted with $s/(\beta\cdot\mathrm{efficiency})$, where $\beta = \mathrm{p/E}$. The energy spectra were determined for $z > 0.225$.
Systematic errors of the fitting procedure were estimated by varying the width of the K^{*+} signal in the data and testing the method with simulated events. Uncertainties in the number of K^{*+} mesons are less than 5%. The efficiency was tested by comparing data which were reconstructed with and without using the vertex chamber information. This chamber has a strong influence on the reconstruction efficiency of K_S^0 decay vertices. Nevertheless the results on K^{*+} production agree within 2.2% after efficiency correction. From Monte Carlo studies a systematic error of 12% on the acceptance was estimated. Additional uncertainties originate from the continuum subtraction and errors of the total cross sections (4% for direct $\Upsilon(1S)$ and 8% for $\Upsilon(4S)$ decays). Note that some of these errors are common to all mesons so that they cancel in ratios.
The extrapolation into the unobserved kinematical region $z < 0.225$ was done by fitting an exponential $f(z) = a\cdot\exp(-bz)$ to the data points of $\frac{1}{\beta\sigma_{\mathrm{had}}}\cdot\frac{\mathrm{d}\sigma}{\mathrm{dz}}$ (figure 11 and 12). The results are given in table 5. In the continuum at $\sqrt{s}$=10.45 GeV 20% and in direct $\Upsilon(1S)$ decays 19% of all K^{*+} mesons have an energy $z < 0.225$. The relative error on the contribution from extrapolation was estimated by applying this method to simulated data in the same way as to real data and comparing the extrapolated multiplicity to the Lund predictions for $z < 0.225$. The differences were found to be 5% and 7% in continuum events and direct $\Upsilon(1S)$ decays.
Due to radiative $\Upsilon(2S)$ decays into the $\chi(1P)$ states different contributions of decays into three and two gluons are expected in $\Upsilon(1S)$ and $\Upsilon(2S)$ decays, but the available statistics

Meson		a	b
Cont.:	K^{*+}	8.10 ± 1.18	6.94 ± 0.31
	K^{*0}	11.06 ± 0.78	7.73 ± 0.16
	ρ^0	7.94 ± 0.83	6.70 ± 0.22
	ω	14.1 ± 5.4	8.81 ± 0.88
$\Upsilon(1S)$:	K^{*+}, $\Upsilon(1S)$	37.6 ± 12.2	10.74 ± 0.84
	K^{*0}	38.3 ± 3.8	10.49 ± 0.29
	ρ^0	35.6 ± 8.2	11.17 ± 0.72
	ω	30.2 ± 19.0	10.75 ± 1.36
$\Upsilon(4S)$:	K^{*+}	$--$	$--$
	K^{*0}	137 ± 71	16.3 ± 2.1
	ρ^0	177 ± 196	17.4 ± 4.0
	ω	$--$	$--$

Table 5: The parameters a and b of the function $a \cdot e^{-bz}$ from fits to the z spectra of vector mesons from continuum (10.45 GeV) events, direct $\Upsilon(1S)$ and $\Upsilon(4S)$ decays (figures 11 to 14).

does not allow to disentangle possible minor differences of the production of vector mesons in two and three gluon decays. However the comparison of the results from direct $\Upsilon(1S)$ and $\Upsilon(2S)$ decays offers a good tool to study systematic errors of the analysis as the ratio $\sigma_{dir}/\sigma_{q\bar{q}}$ changes from 2.0 to 0.8 for data taken at the $\Upsilon(1S)$ and $\Upsilon(2S)$ resonance. Within the given uncertainties the results of all vector mesons agree for direct $\Upsilon(1S)$ and $\Upsilon(2S)$ decays indicating no additional systematic uncertainties.

4.4 The K^{*0} analysis

The same signal shape as for the charged isospin partner was applied. As the mass resolution is better (only two charged tracks are combined to find K^{*0} mesons) Γ_0 was only increased to $53\,MeV/c^2$. Mesons were considered in the mass range from 764 to $1029\,MeV/c^2$ ($\pm 2.5 \cdot \Gamma_0$). Combinations of oppositely charged kaon and pion candidates show in its mass spectrum besides a K^{*0} signal contributions from other resonances. The hadrons ϕ, K^0_S, Λ, ω and ρ^0 as well as a K^{*0} reflection due to an interchange of the particle identities of its decay products were taken into account.

The contribution from a ϕ reflection due to the misidentification of one of the charged kaons as a pion was determined from data. If a pion candidate also fulfilled the kaon hypotheses the invariant K^+K^- mass was plotted. The number of ϕ mesons was calculated by a fit to this mass spectrum and corrected for the identification probabilities. Also the shape of the ϕ reflection in the $K^+\pi^-$ mass spectrum was determined from data. This procedure was repeated for all z bins in every data sample, so that the ϕ contribution could be subtracted before fitting the $K^+\pi^-$ mass spectrum.

A similar method was applied to subtract the K^0_S reflection. Contributions from Λ baryons turned out to be negligible.

A reflection from the decay $\omega \to \pi^+\pi^-\pi^0$, where a charged pion is identified as a kaon, gives

no distinct structure in the mass spectrum, because it overlaps with the maximum of the combinatorial background. Therefore no special treatment of the ω was necessary.

The ρ^0 contribution in the $K^+\pi^-$ mass spectrum due to an erroneous identification of a pion as a kaon was determined by fitting the amplitude of the ρ^0 reflection in the $K^+\pi^-$ spectrum, while its momentum dependent shape was derived from Monte Carlo.

The K^{*0} self reflection was restricted to a negligible level by accepting only those $K^+\pi^-$ combinations, for which the product of the identification likelihoods was larger than the product with interchanged particle hypotheses.

The combinatorial background shows a more complex structure than in the K^{*+} case, as additional contributions due to particle misidentification arise. Fitting was possible with a function consisting of a threshold factor times a polynomial times an exponential with in total six free parameters [5]. The fit procedure was applied to the mass range between 0.65 and $1.5\,GeV/c^2$. The measured energy spectrum covers the range $z > 0.2$. The K^{*0} signal in direct $\Upsilon(1S)$ decays is shown in figure 5 where the same weighting as explained in the previous section was applied.

The systematic uncertainties were estimated similar as described for the K^{*+} analysis by performing Monte Carlo studies and varying the signal shape. Furthermore the K^{*0} analysis was repeated after the ρ^0 measurement described in the following section, when a subtraction of the ρ^0 contribution was possible without fitting. In total the error for the fitting procedure was determined to be 10% in the range $0.2 < z < 0.225$ and 5% for $z > 0.225$. The systematic error on the efficiency amounts to 7%. Additional uncertainties are due to the total hadronic cross sections and the scaling of the continuum.

To extrapolate the z spectra from z=0.2 to the kinematical limit an exponential was used as in the K^{*+} analysis (figures 11, 12 and 13). However for the continuum data a structure visible in the K^{*0} spectrum around z=0.32, which is not reproduced in simulated events, deviated from smooth behaviour. This enhancement may be due to D decays, which concentrate in this z region, but the source could not be identified unambiguously. Therefore the region $0.25 < z < 0.40$ was excluded from the fit to the continuum data. To estimate the systematic error of the extrapolation also the function $f(z) = a \cdot \exp(-bz) + c \cdot \exp(-dz^2)$ was fitted to the continuum data (excluding $0.25 < z < 0.40$) (table 6) and the mean value of both extrapolations was used to calculate the K^{*0} multiplicities. In the continuum ($\Upsilon(1S)$, $\Upsilon(4S)$) 12%

Meson	a	b	c	d
Cont.: K^{*0}	1550 ± 3150	33.7 ± 8.7	1.46 ± 0.15	6.75 ± 0.32

Table 6: Parameters of the function $ae^{-bz} + ce^{-dz^2}$ fitted to the continuum data (10.45 GeV) for K^{*0} mesons (fig. 11).

(3%, 25%) of the K^{*0} rate originates from the extrapolation with a systematic uncertainty of 50% (7%, 20%).

4.5 The ρ^0 analysis

In events simulated with Lund 6.3 the mass distribution of ρ^0 mesons is different from the implemented nonrelativistic Breit-Wigner function. This difference is explained by phase space

effects and correlations with other particles in the fragmentation process which influence the ρ^0 mass. The width of the other vector mesons is too small to show a similar effect. The ρ^0 shape in Lund 6.3 depends on the ρ^0 momentum and on the simulated event type (direct $\Upsilon(1S)$-decays and continuum events). In this analysis we used the ρ^0 shape found in events simulated according to Lund 6.3 after a full detector simulation to determine the number of ρ^0 mesons in data.

Recently evidence for a shift of the ρ^0 mass for mesons produced inclusive in e^+e^- annihilations towards lower values compared to the standard parameters has been claimed. In hadronic Z^0 decays the shift was found to be $(13 \pm 2)\,MeV/c^2$ [10], but may even be as large as $40\,MeV/c^2$ [11]. It has been argued that the origin may be due to Bose-Einstein correlations [12], but up to now it is not understood. Like other analyses of fragmentation in e^+e^- annihilation [13] we do not observe a mass shift, but due to the high background below the ρ^0 signal we are not able to determine details of the mass spectrum of this vector meson from data on fragmentation. The main difference between this analysis, results from $\sqrt{s} \approx 30\,GeV$ and Z^0 decays is the experimental accessible ρ^0 energy ranging from $z > 0.2$ to $z > 0.1$ and $z > 0.05$, respectively. The mass shift may be restricted to very low z values similar as observed in photon and hadron induced ρ^0 production [14], so that it does not appear for $z > 0.2$. Further studies of LEP data will help to clarify this problem. From our data one can certainly exclude a shift of the order of $40\,MeV/c^2$. Nevertheless the analysis was repeated with arbitrary mass shifts of -10 and -20 MeV/c^2. For example in the continuum data an increase of the ρ^0 multiplicity of 3.3% respectively 5.4% was observed, which is well below the quoted systematic error in this analysis.

Many resonances and a large combinatorial background contribute to the visible $\pi^+\pi^-$ mass spectrum. The Monte Carlo predictions are shown in figure 6. In contrast to simulations the data also show the resonance $f_0(975)$ (figure 7). Inclusive multiplicities and z spectra of this scalar meson were determined in parallel to the ρ^0 analysis and are published in [15].

The different components of the $\pi^+\pi^-$ mass spectrum were treated in the following manner. The reflection from K^{*0} mesons due to misidentification of charged kaons as pions is most problematic as it overlaps with the ρ^0 signal. While shape and probability of the reflection were determined from simulations the number of K^{*0} mesons and their momentum distribution were taken from the measurements discussed in the preceding paragraph. The K^{*0} reflection was subtracted from the $\pi^+\pi^-$ mass spectrum without fitting or relying on any fragmentation model.

The shape of the $\pi^+\pi^-$ mass spectrum from the decay $\omega \to \pi^+\pi^-\pi^0$ was taken from simulated events and the number of ω mesons was included as a free parameter in the final fits. The decay mode $\omega \to \pi^+\pi^-$ with a branching ratio of 2.2% and its possible interference with the ρ^0 decay were neglected.

Contributions from K^0_S decays were derived by including an appropriate Gaussian in the fitting procedure. A reflection from Λ baryons was not observed in the data.

Contributions from ϕ and η' mesons do not play any role as the analysis was restricted to invariant $\pi^+\pi^-$ masses above $0.45\,GeV/c^2$. In this range the η meson only contributes via its decay $\eta \to \pi^+\pi^-\gamma$, which was treated in the same manner as the ω meson.

To estimate the large combinatorial background we used the mass spectrum of like-sign pion candidates $m(\pi^\pm\pi^\pm)$, where every entry was weighted with the ratio of the numbers of possible combinations $n(\pi^+\pi^-)/[n(\pi^+\pi^+) + n(\pi^-\pi^-)]$ in its event. A comparison of like and unlike-sign combinations is shown in figure 7. According to simulations the weighted $\pi^\pm\pi^\pm$ combinations describe the combinatorial background with an accuracy of better than 10%. Figure 8 displays the data shown in figure 7 after subtraction of the weighted like-sign pairs. The $f_0(975)$ meson is clearly visible at $m(\pi^+\pi^-) = 975\,MeV/c^2$. The negative entries close to threshold are due to Bose-Einstein correlations which lead to an excess of like-sign pion pairs compared to unlike-sign combinations at low values of invariant masses $m(\pi^+\pi^-)$.

The remaining combinatorial background can be fitted with a second order polynomial. The final fits were performed in the mass interval from 0.45 to $1.2\,GeV/c^2$ (fig. 8) and the ρ^0 energy spectra for $z > 0.2$ determined from data.

To estimate the systematic error of the fitting procedure and especially the sensitivity of the results on the ρ^0 shape the fits were repeated with a nonrelativistic Breit-Wigner mass distribution. Additional tests with Monte Carlo events and arbitrary variations of the K^{*0} reflection of $\pm 20\%$ show that the uncertainty on the fitted number of ρ^0 mesons is less than 6%. The systematic error on the acceptance was determined to be 7%. The additional uncertainties on the scaling of the continuum and the Υ cross sections are the same as in the K^* analyses.

The ρ^0 spectra $\frac{1}{\beta\sigma_{had}} \cdot \frac{d\sigma}{dx}$ were again fitted with an exponential and extrapolated to the kinematical threshold. In the continuum ($\Upsilon(1S)$, $\Upsilon(4S)$) 19% (21%, 48%) of the ρ^0 multiplicity originate from the extrapolation (figures 11, 12 and 14). The relative uncertainties on these fractions were estimated to be 40%, 7% and 20% respectively.

4.6 The ω analysis

The visible width of the ω signal is dominated by detector resolution effects. In this analysis the signal was described by a convolution of the detector response function with a Breit-Wigner mass distribution, where width and mass value were taken from reference [7].

The high combinatorial background in combinations of three pions complicates the isolation of an ω signal in the $\pi^+\pi^-\pi^0$ mass spectrum. This problem becomes even more severe when neutral pions are reconstructed by combining two photon candidates detected in the electromagnetic calorimeter. Because of the large number of photons in a typical event (≈ 7) and the limited spatial and energy resolution of the ARGUS calorimeter π^0 mesons can be identified only with a huge background [16]. One way out is to use only one photon candidate from the calorimeter and demanding for the other photon a conversion into an e^+e^- pair in the detector material. Figure 9 shows the invariant mass of $\pi^+\pi^-\pi^0$ combinations with the use of converted photons. An ω signal is visible and proves for the first time the production of this vector meson in e^+e^- annihilation. However this method has two disadvantages: only ω mesons with momenta above $2\,GeV/c$ can be reconstructed, so that most of the inclusive multiplicity would rely on the extrapolation to low momenta. Furthermore the statistics is not sufficient to separate continuum events and Υ decays.

Therefore we used two photon candidates from the calorimeter to reconstruct π^0 mesons as described above. Corresponding $\pi^+\pi^-\pi^0$ mass spectra are shown in figure 10. In the data as well as in simulated events the background shows a smooth behaviour and was parametrized by an exponential times a straight line. Fits were applied in the range from 0.68 to $0.88\,GeV/c^2$. A fit including an ω contribution gives a $\chi^2/NDoF = 30.8/36$ (fig. 10(a)) while neglecting any ω production results in $\chi^2/NDoF = 100.2/37$ (fig. 10(b)). When combinations of two photons not compatible with π^0 mesons are used the spectrum shows no evidence for a signal (fig. 10(c)).

The systematic uncertainty of the fits was estimated by studying Monte Carlo data, comparing different time periods of data taking (the background shape might be influenced by different conditions of the calorimeter) and by repeating the analysis with a cut in the Dalitz distribution of the three pion system, where pions from ω decays are more centered than random combinations due to their relative angular momentum. With this cut the signal to background ratio improves by a factor 1.9, but the significance of the ω signal stays the same. Therefore the Dalitz cut was omitted in the final analysis. These comparisons result in a systematic error of 15% for the fitting procedure. The uncertainty of the efficiency was determined by similar methods as described in the other analyses and found to be 10%. Additional uncertainties arise from the continuum scaling and resonance cross sections which have been mentioned above.
Energy spectra of ω mesons could be determined from data in the interval $0.2 < z < 0.85$ (figure 11 and 12). The extrapolation down to the kinematical threshold and above z=0.85 correspond in the continuum and direct $\Upsilon(1S)$ decays to 24% and 18% of the total multiplicity with relative errors of 40% and 7% respectively.

5 Discussion of results

The z spectra of vector mesons measured in this analysis are plotted in fig. 11 to 14 for the continuum data, direct $\Upsilon(1S)$ and $\Upsilon(4S)$ decays. Only statistical uncertainties are shown. The fits used to extrapolate into the unmeasured z regions are overlayed to the data. They have been described above, where also the contributions of the extrapolations to the total multiplicities are given.
For comparison we include data published by the CLEO collaboration [17], which are the only measurements available so far in the energy region of the Υ resonances. In contrast to this analysis the CLEO results for continuum events were not corrected for initial state radiation of photons, which gives rise to small changes in the z spectra (compare section 4). The overall agreement between both experimental results is satisfactory if one considers the systematic and statistical uncertainties. However the CLEO data systematicaly tend to larger values than our measurement, which is most obvious for the K^{*+} spectrum in the continuum and for ρ^0 mesons from direct $\Upsilon(1S)$ decays. The latter can be explained partly by the method used by the CLEO collaboration to extrapolate measured continuum data to the $\Upsilon(1S)$ energy. For the K^{*+} production in the continuum and direct $\Upsilon(1S)$ decays at low z a major disagreement between the CLEO results and the extrapolated ARGUS data exists. Since our fit to the invariant $K^0_s\pi^+$ mass becomes unreliable at these low z values ARGUS has restrained from presenting data in this region.
Besides the results from ARGUS and CLEO the figures 11 to 14 show predictions from Lund 7.3. Note that Lund 7.3 does not differ from Lund 6.3 in the description of the fragmentation process, but in the particle table many branching ratios for charmed hadrons have been updated or added in Lund 7.3. In general the simulated multiplicities are too high in direct $\Upsilon(1S)$ decays. The slope of the z spectra from Monte Carlo agrees with the ARGUS data in the continuum, whereas Lund and data differ significantly in direct $\Upsilon(1S)$ decays.
The vector meson multiplicities for continuum events, direct $\Upsilon(1S)$ and $\Upsilon(4S)$ decays are shown in the tables 7 to 9, where the first error is due to statistical and the second due to systematic uncertainties. The upper limit for ω production in $\Upsilon(4S)$ decays corresponds to

a confidence level of 90%. It was obtained by assuming that the z spectrum for ω mesons is equal to the ρ^0 spectrum in these decays. In the same way the K^{*0} spectrum was used to determine the K^{*+} multiplicity in $\Upsilon(4S)$ decays. For completion we have included the results for ϕ production in continuum events and direct $\Upsilon(1S)$ decays from ref. [18], where the continuum multiplicity has been rescaled from $\sqrt{s}$=9.46 GeV to 10.45 GeV. Reference [19] was used for $\Upsilon(4S)$ decays. Measurements by the CLEO collaboration [17] and simulations according to Lund 7.3 and UCLA 7.31 [20] are added to table 7. Data from direct $\Upsilon(1S)$ decays (table 8) are only compared to Lund 7.3, as the UCLA model is not yet capable of simulating Υ decays. Table 10 lists the vector meson spectra measured in this analysis.

Continuum (10.45 GeV)				
Meson	ARGUS	CLEO	Lund 7.3	UCLA 7.31
ω	$0.295 \pm 0.047 \pm 0.060$	- - -	0.44	-
ρ^0	$0.326 \pm 0.015 \pm 0.038$	0.50 ± 0.09	0.55	0.43
K^{*0}	$0.292 \pm 0.007 \pm 0.029$	0.38 ± 0.09	0.35	0.29
K^{*+}	$0.246 \pm 0.015 \pm 0.031$	0.45 ± 0.08	0.43	0.35
ϕ	$0.044 \pm 0.002 \pm 0.002$	0.08 ± 0.02	0.072	0.052

Table 7: The vector meson multiplicities in continuum events measured by ARGUS and CLEO [17] and simulation results according to the Lund and UCLA models. The ARGUS results are radiation corrected, the simulations do not include initial state radiation of photons.

Direct $\Upsilon(1S)$ decays			
Meson	ARGUS	CLEO	Lund 7.3
ω	$0.314 \pm 0.109 \pm 0.058$	- - -	0.64
ρ^0	$0.333 \pm 0.025 \pm 0.034$	0.57 ± 0.14	0.74
K^{*0}	$0.328 \pm 0.010 \pm 0.031$	0.80 ± 0.30	0.46
K^{*+}	$0.291 \pm 0.030 \pm 0.040$	0.42 ± 0.15	0.46
ϕ	$0.055 \pm 0.002 \pm 0.003$	0.15 ± 0.05	0.072

Table 8: The vector meson multiplicities in direct $\Upsilon(1S)$ decays measured by ARGUS and CLEO [17] and simulation results according to the Lund model.

$\Upsilon(4S)$ decays	
Meson	ARGUS
ω	< 0.81 (90% CL)
ρ^0	$0.417 \pm 0.083 \pm 0.065$
K^{*0}	$0.292 \pm 0.032 \pm 0.040$
K^{*+}	$0.364 \pm 0.108 \pm 0.047$
ϕ	$0.078 \pm 0.006 \pm 0.007$

Table 9: The vector meson multiplicities in $\Upsilon(4S)$ decays measured by ARGUS.

z Interval	Cont.(10.45 GeV)	Υ(1S) direct	Υ(4S) direct
K^{*+} mesons:	$1/(\beta\sigma_{had}) \cdot d\sigma/dz$		$1/\sigma_{dir} \cdot d\sigma/dz$
0.225-0.275	$0.95 \pm 0.21 \pm 0.12$	$2.92 \pm 0.55 \pm 0.40$	$3.43 \pm 0.75 \pm 0.52$
0.275-0.325	$1.26 \pm 0.12 \pm 0.16$	$1.16 \pm 0.31 \pm 0.16$	$0.03 \pm 0.60 \pm 0.01$
0.325-0.375	$0.64 \pm 0.11 \pm 0.08$	$0.95 \pm 0.18 \pm 0.13$	$0.62 \pm 0.37 \pm 0.09$
0.375-0.425	$0.505 \pm 0.081 \pm 0.064$	$0.54 \pm 0.13 \pm 0.07$	$0.39 \pm 0.31 \pm 0.06$
0.425-0.475	$0.398 \pm 0.065 \pm 0.050$	$0.305 \pm 0.092 \pm 0.041$	$-0.10 \pm 0.24 \pm 0.02$
0.475-0.525	$0.271 \pm 0.061 \pm 0.034$	$0.207 \pm 0.073 \pm 0.028$	$-0.11 \pm 0.20 \pm 0.02$
0.525-0.600	$0.182 \pm 0.034 \pm 0.023$	$0.052 \pm 0.037 \pm 0.007$	$-0.16 \pm 0.12 \pm 0.02$
0.600-0.700	$0.062 \pm 0.022 \pm 0.008$	$0.041 \pm 0.021 \pm 0.005$	$0.082 \pm 0.071 \pm 0.013$
0.700-0.800	$0.076 \pm 0.011 \pm 0.010$	$0.009 \pm 0.011 \pm 0.001$	$-0.106 \pm 0.040 \pm 0.016$
0.800-1.000	$0.0095 \pm 0.0034 \pm 0.0010$	$0.0045 \pm 0.0031 \pm 0.0006$	$-0.021 \pm 0.010 \pm 0.003$
K^{*0} mesons:	$1/(\beta\sigma_{had}) \cdot d\sigma/dz$		$1/\sigma_{dir} \cdot d\sigma/dz$
0.200-0.225	$2.28 \pm 0.15 \pm 0.29$	$5.84 \pm 0.47 \pm 0.80$	$2.12 \pm 0.39 \pm 0.29$
0.225-0.250	$1.52 \pm 0.11 \pm 0.12$	$3.44 \pm 0.26 \pm 0.33$	$2.79 \pm 0.34 \pm 0.33$
0.250-0.275	$1.52 \pm 0.09 \pm 0.12$	$1.78 \pm 0.19 \pm 0.17$	$1.04 \pm 0.36 \pm 0.12$
0.275-0.300	$1.31 \pm 0.09 \pm 0.11$	$1.67 \pm 0.15 \pm 0.16$	$0.76 \pm 0.39 \pm 0.09$
0.300-0.325	$1.35 \pm 0.08 \pm 0.11$	$1.40 \pm 0.14 \pm 0.13$	$0.38 \pm 0.31 \pm 0.04$
0.325-0.350	$1.11 \pm 0.08 \pm 0.09$	$1.26 \pm 0.12 \pm 0.12$	$0.39 \pm 0.27 \pm 0.05$
0.350-0.375	$0.690 \pm 0.072 \pm 0.056$	$0.84 \pm 0.10 \pm 0.08$	$0.36 \pm 0.25 \pm 0.04$
0.375-0.400	$0.555 \pm 0.066 \pm 0.045$	$0.796 \pm 0.092 \pm 0.076$	$0.42 \pm 0.23 \pm 0.05$
0.400-0.450	$0.418 \pm 0.036 \pm 0.034$	$0.477 \pm 0.054 \pm 0.045$	$0.13 \pm 0.13 \pm 0.02$
0.450-0.500	$0.314 \pm 0.029 \pm 0.025$	$0.194 \pm 0.038 \pm 0.018$	$0.10 \pm 0.10 \pm 0.01$
0.500-0.600	$0.195 \pm 0.015 \pm 0.016$	$0.144 \pm 0.018 \pm 0.014$	$0.032 \pm 0.052 \pm 0.004$
0.600-0.700	$0.0893 \pm 0.0090 \pm 0.0072$	$0.035 \pm 0.010 \pm 0.003$	$0.033 \pm 0.031 \pm 0.004$
0.700-0.850	$0.0213 \pm 0.0043 \pm 0.0017$	$0.0145 \pm 0.0038 \pm 0.0014$	$0.030 \pm 0.013 \pm 0.004$
0.850-1.000	$0.0048 \pm 0.0014 \pm 0.0004$	$0.0018 \pm 0.0013 \pm 0.0002$	$-0.0024 \pm 0.0043 \pm 0.0003$
ρ^0 mesons:	$1/(\beta\sigma_{had}) \cdot d\sigma/dz$		$1/\sigma_{dir} \cdot d\sigma/dz$
0.200-0.225	$2.09 \pm 0.32 \pm 0.18$	$3.37 \pm 0.62 \pm 0.34$	$2.97 \pm 0.94 \pm 0.36$
0.225-0.250	$1.65 \pm 0.25 \pm 0.14$	$1.81 \pm 0.46 \pm 0.18$	$2.32 \pm 0.80 \pm 0.28$
0.250-0.275	$1.10 \pm 0.20 \pm 0.10$	$1.99 \pm 0.38 \pm 0.20$	$1.69 \pm 0.70 \pm 0.21$
0.275-0.300	$1.01 \pm 0.17 \pm 0.09$	$1.34 \pm 0.32 \pm 0.13$	$1.46 \pm 0.63 \pm 0.18$
0.300-0.325	$1.09 \pm 0.15 \pm 0.09$	$1.26 \pm 0.26 \pm 0.13$	$0.22 \pm 0.58 \pm 0.03$
0.325-0.350	$0.84 \pm 0.13 \pm 0.07$	$1.06 \pm 0.21 \pm 0.11$	$0.55 \pm 0.52 \pm 0.07$
0.350-0.375	$0.75 \pm 0.11 \pm 0.07$	$0.73 \pm 0.17 \pm 0.07$	$0.09 \pm 0.42 \pm 0.01$
0.375-0.400	$0.559 \pm 0.090 \pm 0.049$	$0.38 \pm 0.16 \pm 0.04$	$0.28 \pm 0.41 \pm 0.03$
0.400-0.450	$0.387 \pm 0.061 \pm 0.034$	$0.354 \pm 0.088 \pm 0.035$	$0.34 \pm 0.23 \pm 0.04$
0.450-0.500	$0.369 \pm 0.045 \pm 0.032$	$0.231 \pm 0.064 \pm 0.023$	$-0.25 \pm 0.19 \pm 0.03$
0.500-0.600	$0.217 \pm 0.023 \pm 0.019$	$0.047 \pm 0.029 \pm 0.005$	$0.032 \pm 0.087 \pm 0.004$
0.600-0.700	$0.120 \pm 0.015 \pm 0.010$	$0.006 \pm 0.015 \pm 0.001$	$-0.027 \pm 0.038 \pm 0.003$
0.700-0.850	$0.0441 \pm 0.0079 \pm 0.0038$	$0.0202 \pm 0.0072 \pm 0.0020$	$0.018 \pm 0.025 \pm 0.002$
0.850-1.000	$0.0113 \pm 0.0032 \pm 0.0010$	$-0.0030 \pm 0.0022 \pm 0.0003$	$-0.0049 \pm 0.0086 \pm 0.0006$
ω mesons:	$1/(\beta\sigma_{had}) \cdot d\sigma/dz$		
0.200-0.250	$2.29 \pm 0.78 \pm 0.41$	$3.15 \pm 2.38 \pm 0.58$	- -
0.250-0.300	$0.65 \pm 0.38 \pm 0.12$	$1.91 \pm 0.83 \pm 0.35$	- -
0.300-0.350	$1.08 \pm 0.24 \pm 0.19$	$0.53 \pm 0.40 \pm 0.10$	- -
0.350-0.400	$0.42 \pm 0.14 \pm 0.07$	$0.28 \pm 0.23 \pm 0.05$	- -
0.400-0.500	$0.323 \pm 0.053 \pm 0.057$	$0.343 \pm 0.066 \pm 0.063$	- -
0.500-0.600	$0.098 \pm 0.033 \pm 0.017$	$0.065 \pm 0.032 \pm 0.012$	- -
0.600-0.700	$0.033 \pm 0.023 \pm 0.006$	$0.021 \pm 0.018 \pm 0.004$	- -
0.700-0.850	$0.014 \pm 0.010 \pm 0.002$	$0.007 \pm 0.008 \pm 0.001$	- -

Table 10: Inclusive cross sections of vector mesons. The continuum results are in the lowest order of QED (radiation corrected).

In the following sections we will first use the results from direct Υ(1S) decays to determine fragmentation characteristics without uncertainties due to charm decays or leading quark effects. In a second step Lund 7.3 with modified parameters will be compared to the experimental data.

5.1 Comparison of ω and ρ^0 production

The production of ω mesons, which has been observed for the first time in e^+e^- annihilation, and ρ^0 mesons are naively expected to be equal in fragmentation since these vector mesons have the same quark content, the same spin and nearly equal masses. They differ only by their isospin. The ratio of the ω and ρ^0 inclusive cross section as a function of the scaled energy z is shown in fig. 15 for direct Υ(1S) decays, where no charm decays contribute to the meson multiplicities. Within the statistical uncertainties no z dependence is observed. Fitting a constant results in $n(\omega)/n(\rho^0)_{\Upsilon(1S),fit} = 0.85 \pm 0.19 \pm 0.14$. In table 11 the ratio of the multiplicities $n(\omega)/n(\rho^0)$ for continuum data, direct Υ(1S) decays and mean values from both event types are given. The results of the present experiment for direct Υ(1S)

	$n(\omega)/n(\rho^0)$	
Event type	$0.20 < z < 0.85$	incl. extrap.
Continuum	$0.85 \pm 0.14 \pm 0.14$	$0.90 \pm 0.15 \pm 0.14$
Υ(1S) direct	$0.97 \pm 0.35 \pm 0.16$	$0.94 \pm 0.33 \pm 0.15$
Mean	$0.87 \pm 0.13 \pm 0.14$	$0.91 \pm 0.14 \pm 0.14$

Table 11: The ratio of ω and ρ^0 production in continuum events, in direct Υ(1S) decays and the mean value from both event types only from measured data and including the extrapolation into the not observed z regions.

decays and continuum events are in good agreement with data from soft pp interactions [21] of $n(\omega)/n(\rho^0) = 1.02 \pm 0.08$. Lund 7.3 predicts $n(\omega)/n(\rho^0) = 0.95$, if differences between simulated and measured η' multiplicity [15] are taken into account as 30% of these mesons decay into ρ^0 mesons.

5.2 The vector meson suppression

Combining the results of this analysis with ARGUS data on the production of ϕ mesons [18] and pseudoscalar particles [15,16,22] in direct Υ(1S) decays we obtain multiplicities for nearly all particles in the pseudoscalar and vector meson nonets. Only the multiplicities of charged ρ mesons have not been measured yet, but the production rate in the fragmentation is expected to be twice the ρ^0 rates from simple isospin arguments.
This collection of data allows to calculate the relative production of vector mesons and pseudoscalars without fitting model parameters. The direct Υ(1S) decays have the additional advantage to produce at most very few charm particles [4], so that uncertainties due to charmed hadron branching ratios do not influence this data. Note however that systematic uncertainties remain due to the unknown production of tensor and scalar mesons which have not yet been measured with sufficient precision.

Vector meson to pseudoscalar ratios are listed in table 12, where the ρ^0 is compared to $\pi^\pm$ instead of π^0 mesons to minimize the experimental uncertainties. The ARGUS and CLEO [17]

Ratio	ARGUS	CLEO	Lund 7.3
$\rho^0/\pi^\pm$	0.044 ± 0.006	0.066 ± 0.016	0.095
K^{*0}/K^0	0.318 ± 0.035	0.76 ± 0.30	0.53
K^{*+}/K^+	0.320 ± 0.056	0.57 ± 0.23	0.52

Table 12: The relative production rates for vector meson and pseudoscalars in direct $\Upsilon(1S)$ decays from ARGUS measurements, CLEO results [17] and predictions from Lund 7.3.

results agree within errors. The low experimental uncertainties of the ARGUS data reveal a systematic difference to the Lund model, which significantly overestimates all ratios. Figure 16 shows the ρ^0/π^+ ratio as a function of the scaled energy z. Within errors no dependence of the ratio on z is observed. The difference between the ratio in this figure and the number in table 12 is due to the different kinematical range of the z spectra. For pions from direct $\Upsilon(1S)$ decays it extends down to z=0.03 while the ρ meson spectrum stops at z=0.16.
Very often a ratio V/(V+P), where mesons from secondary decays are not included, is used to describe the relative abundancy of vector mesons and pseudoscalars in fragmentation. Using the ARGUS data and branching ratios from ref. [7] a ratio $V/(V+P)_K$ for K^* and K mesons and a similar parameter $V/(V+P)_\pi$ for mesons without s quarks were calculated:

$$\left(\frac{V}{V+P}\right)_K = \frac{n(K^{*0}) + n(K^{*+})}{n(K^0) + n(K^+) - 2 \cdot 0.84 \cdot n(\phi)} \quad ,$$

$$\left(\frac{V}{V+P}\right)_\pi = \frac{n(\rho^0) + n(\omega) - n(\mathrm{Res}, \rho^0, \omega)}{n(\rho^0) + n(\omega) + n(\pi^0) + n(\eta) + n(\eta') - n(\mathrm{decay})} \quad .$$

Here the measured multiplicities are symbolized with n. In the second formula $n(\mathrm{Res}, \rho^0, \omega)$ sums up the ρ^0 and ω contributions from ϕ and η' decays while n(decay) comprises the number of ρ^0, ω, π^0 and η mesons produced in decays of ϕ, K^*, ρ, ω, K^0, η and η' mesons as well as Λ baryons. For η and η' mesons a mixing angle of -20^0 [7] and (s/u)=0.3 was used to calculate the fraction of both mesons produced from $u\bar{u}$ and $d\bar{d}$ quark pairs in fragmentation.
All multiplicities stem from measurements, the only assumption concerns the production of charged ρ mesons as mentioned above. Decays of heavier baryons were not taken into account as their multiplicities are small in direct $\Upsilon(1S)$ decays [23,24]. The results for V/(V+P) are given in table 13. The numbers in the second column were obtained by applying the same method to calculate V/(V+P) from simulated Lund 7.3 events. The numbers agree within 10% with the Lund parameters used in the simulation (third column). From this we conclude that the calculation provides a good estimate for V/(V+P).
The values V/(V+P) from data are significantly smaller than the parameters used in the Lund model so that the production of vector mesons is overestimated in the simulation (compare also table 8). This has been observed recently also in hadronic Z^0 decays [25]. If the suppression of s quarks is kept constant to the default value, the measurement of K^{*+} production could only be described with the Lund model by setting the parameter $V/(V+P) = 0.36 \pm 0.05$, which is in very good agreement to our result. The analysis of pp

Ratio	Data	Lund eff.	Lund para.
$V/(V+P)_K$	0.335 ± 0.034	0.56	0.60
$V/(V+P)_\pi$	0.208 ± 0.041	0.45	0.50

Table 13: The parameter V/(V+P) for mesons with (K) and without (π) s quark from multiplicities in direct $\Upsilon(1S)$ decays. The results from data and simulated events as well as the used Lund parameters are shown.

interactions support our model independent conclusions: The LEBC collaboration determined $V/(V+P) = 0.41 \pm 0.03$ from K^* and K production. Also in π^+p [26] and deep inelastic νp and $\bar{\nu}$p scattering [27] the ρ^0 production in the fragmentation regime was observed to be suppressed compared to the Lund model. Studies on intermittency [28] indirectly confirm our results on vector meson production.

5.3 The suppression of s quarks

Similar to the previous section our data can be used to determine the relative production probability for s compared to u quarks in fragmentation. In the string picture quarks are created when strings break up, where s quarks are suppressed due to their high mass. The commonly used parameter (s/u) describes the relative abundancy of quark flavours produced by string breaking: u:d:s=1:1:(s/u). Neglecting vector mesons originating from secondary decays (s/u) can be determined from the production rates of vector mesons:

$$\left(\frac{s}{u}\right) = \frac{n(K^{*0})}{n(\rho^0) + n(\omega)} = \frac{n(K^{*+})}{n(\rho^0) + n(\omega)}$$

$$= \frac{2 \cdot n(\phi)}{n(K^{*0})} = \frac{2 \cdot n(\phi)}{n(K^{*+})} = \sqrt{\frac{2 \cdot n(\phi)}{n(\rho^0) + n(\omega)}}.$$

These relations do not hold for quarks produced via a virtual photon or Z^0 boson, where the electroweak coupling determines the flavour ratios of leading quarks. In Z^0 decays u and s quarks are produced with approximately equal probabilities. This is in contrast to direct $\Upsilon(1S)$ decays. Here the quarks are created only by the strong interaction.
Table 14 shows multiplicity ratios as measured at ARGUS and CLEO [17] and as simulated with Lund 7.3. To minimize experimental uncertainties $n(\rho^0) + n(\omega)$ was replaced by $2 \cdot n(\rho^0)$. Within the given errors the values of CLEO and ARGUS agree, while the ratios obtained from Lund are significantly lower than measured in this analysis. However the results on V/(V+P) complicate the determination of (s/u) and comparisons to Lund as the vector meson suppression depends on the quark content of the hadron and was found to be different in data and the Lund model. The multiplicity ratios have to be corrected for V/(V+P) to calculate the s quark suppression. Choosing $K^{*0}/2\rho^0$ and $2\phi/K^{*+}$ as independent ratios from our measurements and correcting for secondary decays (ϕ and η' decays to ρ^0 mesons) one obtains

$$\left(\frac{s}{u}\right) = \frac{1}{2} \cdot \frac{n(K^{*0})}{n(\rho^0) - n(\mathrm{Res}, \rho^0)} \cdot \frac{V/(V+P)_\pi}{V/(V+P)_K} = \frac{2 \cdot n(\phi)}{n(K^{*+})}$$

Ratios	ARGUS	CLEO	Lund 7.3
$n(K^{*0})/2 \cdot n(\rho^0)$	$0.492 \pm 0.040 \pm 0.038$	0.70 ± 0.31	0.31
$n(K^{*+})/2 \cdot n(\rho^0)$	$0.437 \pm 0.056 \pm 0.034$	0.37 ± 0.16	0.31
$2 \cdot n(\phi)/n(K^{*0})$	$0.332 \pm 0.017 \pm 0.023$	0.38 ± 0.19	0.31
$2 \cdot n(\phi)/n(K^{*+})$	$0.375 \pm 0.041 \pm 0.026$	0.71 ± 0.35	0.31
$\sqrt{n(\phi)/n(\rho^0)}$	$0.405 \pm 0.017 \pm 0.016$	0.51 ± 0.11	0.31

Table 14: Vector meson multiplicity ratios in direct $\Upsilon(1S)$ decays from ARGUS and CLEO data [17] and from the model Lund 7.3.

Mesons	ARGUS	Lund eff.	Lund para.
K^{*0}, ρ^0	0.355 ± 0.085	0.30	0.30
ϕ, K^{*+}	0.375 ± 0.049	0.31	0.30

Table 15: The s quark suppression (s/u) calculated from the inclusive multiplicities of vector mesons in direct $\Upsilon(1S)$ decays from data and simulated events (Lund 7.3). The last column lists the used Lund parameters.

and achieves the results in table 15. Both experimental results agree very well. The similarity between the last two columns in table 15 proves again the validity of our analysis. The mean value for the s quark suppression is found to be

$$\left(\frac{s}{u}\right) = 0.37 \pm 0.04$$

for vector mesons. This is in excellent agreement with $(s/u) = 0.32 \pm 0.06$ determined in a similar model independent way from baryon multiplicities [23]. The experimental values tend to be higher than (s/u) in the Lund model but given the uncertainties due to the production of yet unmeasured tensor and scalar mesons data and simulation are not in contradiction.
Our result for (s/u) lies between measurements from diffractive pp scattering [21] and pp scattering with high momentum transfers and large z [29], which yield $(s/u) = 0.22 \pm 0.01$ and $(s/u) = 0.55 \pm 0.05$ respectively. This may hint to a dependence of (s/u) on the involved momentum transfer.

5.4 Comparisons between Data and Simulations

We compared predictions from the models Lund 7.3 and UCLA 7.31 to the measurements. Inclusive multiplicities are listed in tables 7 and 8. Unfortunately only the multiplicities for continuum data were available for the UCLA model, so that the Lund simulations could be tested in more details, which was partly shown in the last sections. Here we discuss possible explanations for the observed discrepancies and change model parameters to reproduce the measurements.

Direct $\Upsilon(1S)$ decays

The most obvious difference between the data presented in this analysis and Lund 7.3 concern V/(V+P), which is overestimated by a factor of approximately 2 in the simulation. The measured vector meson suppression (table 13) and s/u=0.37 (table 15) were used instead of the standard parameters to achieve the simulated multiplicities listed in table 16. The ρ^0 rate was corrected for the difference of measured and simulated η' multiplicities [15], as 30% of these mesons decay to ρ^0 mesons. Within the experimental uncertainties data

	Direct $\Upsilon(1S)$ decays		Continuum	
Meson	Data	Lund mod.	Data	Lund mod.
ω	0.314 ± 0.124	0.28	0.295 ± 0.076	0.21
ρ^0	0.333 ± 0.042	0.31	0.326 ± 0.041	0.26
K^{*0}	0.328 ± 0.033	0.32	0.292 ± 0.030	0.26
K^{*+}	0.291 ± 0.050	0.32	0.246 ± 0.034	0.33
ϕ	0.055 ± 0.003	0.059	0.044 ± 0.003	0.065

Table 16: Vector meson multiplicities measured in this analysis and ϕ results from reference [18] (statistical and systematic uncertainties were added in quadrature) and simulated rates according to Lund 7.3 with modified parameters. Details are explained in the text.

and simulations agree very well, although Lund was not used to determine V/(V+P) and (s/u). Multiplicities of pseudoscalar particles predicted with the modified Lund model differ compared to the standard simulation, but the agreement with measured multiplicities for $\pi^{\pm}$, $K^{\pm}$ and K^0_s mesons does not change significantly.
A serious discrepancy between data and Lund 7.3 arises from the shape of the z spectra of vector mesons in direct $\Upsilon(1S)$ decays. In figure 12 the simulated spectra fall off more rapidly than the measured distributions. A similar behaviour for ϕ mesons was noticed in reference [18]. Fitting an exponential $a \cdot e^{-bz}$ to the spectra yields within errors the same b for all vector mesons (table 5). One obtains a mean value of $\overline{b}(\text{data}) = 10.60 \pm 0.25$, while Lund gives $\overline{b}(\text{Lund}) = 14.1$ for the standard and also for our modified version of Lund 7.3. The reason for this difference is not understood. It may be related to the fragmentation of gluons in direct $\Upsilon(1S)$ decays and their string configuration, to the basic fragmentation function or the treatment of interfering gluons. Variations of different parameters did not change the shape of the predicted z spectra as long as the fragmentation function was kept unchanged. Simulations with Lund 7.3 including the production of scalar and tensor mesons (tuned to reproduce our measurements of $f_0(975)$ [15] and D^{**} [30] production) did not reproduce the slope of the z spectra of vector mesons in direct $\Upsilon(1S)$ decays [31]. Probably the observed differences are related not to the fragmentation itself, but to the configuration of the primary gluons. Here the Lund model uses only a simple matrixelement which conserves spin and parity and is also applied to describe the decay of ortho-positronium. An analysis of direct photons from the decay $\Upsilon(1S) \to g\,g\,\gamma$ [32] proved the necessity to take into account QCD corrections, so that one expects important corrections from QCD also for the string configuration of three primary gluons.

Continuum data

In continuum events the production of vector mesons has been measured with small uncertainties at center of mass energies of 10, 29 and 90 GeV. Inclusive multiplicities are given in table 17. To look for energy dependent variations of V/(V+P) or (s/u) we have determined the multiplicity ratios in table 18. Within errors the results do not depend on the center of

Meson	10.45 GeV	29 GeV	90 GeV
ω	0.295 ± 0.076	–	–
ρ^0	0.326 ± 0.041	0.81 ± 0.08	0.83 ± 0.14
K^{*0}	0.292 ± 0.030	0.56 ± 0.06	0.77 ± 0.08
K^{*+}	0.246 ± 0.034	0.64 ± 0.05	0.77 ± 0.08
ϕ	0.0443 ± 0.0031	0.085 ± 0.011	0.086 ± 0.018

Table 17: Vector meson multiplicities in continuum events. The data for 10.45 GeV are from this analysis and reference [18], for 29 GeV from [33] and for 90 GeV from [10] (ρ^0), mean values from [10] and [11] (K^{*0}), mean values from [25] and [34] (K^{*+}) and from [11] (ϕ). All results are corrected for initial state radiation of photons.

Ratio	10.45 GeV	29 GeV	90 GeV
K^{*+}/K^{*0}	0.84 ± 0.12	1.14 ± 0.15	1.00 ± 0.15
K^{*0}/ρ^0	0.90 ± 0.12	0.69 ± 0.10	0.93 ± 0.18
ϕ/K^{*0}	0.15 ± 0.02	0.15 ± 0.03	0.11 ± 0.03
ϕ/ρ^0	0.13 ± 0.02	0.11 ± 0.02	0.10 ± 0.03
K^{*0}/K^0	0.33 ± 0.04	0.39 ± 0.05	0.37 ± 0.05
K^{*+}/K^+	0.29 ± 0.04	0.43 ± 0.04	–
ρ^0/π^+	0.053 ± 0.007	0.079 ± 0.008	–

Table 18: Multiplicity ratios at different center of mass energies. Pseudoscalar production rates at 10.45 GeV were taken from [16,22] and scaled to 10.45 GeV using the Lund model. For 29 GeV ref. [33] and for 90 GeV ref. [35] were used for multiplicities of pseudoscalars.

mass energy. This supports the Lund ansatz to treat the parameters V/(V+P) and (s/u) as independent from the center of mass energy.
Lund 7.3 predicts too many vector mesons for continuum events (compare table 7), but the discrepancies become less severe when the parameters V/(V+P) and (s/u) measured in direct $\Upsilon(1S)$ decays are used (table 16). The remaining differences may be related to uncertainties of charm branching ratios. For example in the modified Lund simulation more than 30% of all ϕ mesons stem from D_s^+ decays, but production and decay of this charmed meson are measured only with very limited accuracy, so that ϕ production in charm decays may easily be overestimated. Up to now unknown ρ^0 production in multi body charm decays may be responsible for the remaining difference of measured and simulated multiplicity in table 16. The shape of the z spectra (figure 11) in data and simulations agree better in continuum

events than in direct $\Upsilon(1S)$ decays.
Simulations with the model UCLA 7.31 yield results very similar to Lund 7.3. Comparisons to our data do not favour one of these models. However a major problem of both models becomes obvious if multiplicities for the same vector meson at different center of mass energies are compared. Table 19 shows multiplicity ratios of results at 29 and 10.45 GeV. The measured ratios are always larger than the predictions, but data and model agree if

Meson	Data	Lund 7.3	UCLA 7.31	Data, $z > 0.325$	Lund 7.3, $z > 0.325$
ρ^0	2.48 ± 0.40	1.74 ± 0.01	1.67 ± 0.01	0.75 ± 0.13	0.64 ± 0.01
K^{*0}	1.92 ± 0.28	1.68 ± 0.01	1.58 ± 0.01	0.70 ± 0.11	0.62 ± 0.01
K^{*+}	2.60 ± 0.41	1.60 ± 0.01	1.52 ± 0.01	0.95 ± 0.16	0.66 ± 0.01
ϕ	1.92 ± 0.28	1.57 ± 0.03	1.52 ± 0.03	–	–

Table 19: Multiplicity ratios of 29 and 10.45 GeV continuum events from measurements and simulations with Lund 7.3 and UCLA 7.31. For comparison results at 29 GeV from ref. [33] and from [36] for $z > 0.325$ have been used.

vector mesons with $z < 0.325$ are excluded from the comparisons. This was done only for the Lund model as no z spectra from UCLA simulations were available. In general the inclusive vector meson spectra from both models agree [20], so that results very similar to the Lund predictions for $z > 0.325$ are expected. Because no averaged z spectra for vector mesons at 29 GeV are available, we used spectra measured by the HRS collaboration [36], which have the smallest statistical uncertainties in this energy region. The ratios do not change significantly for simulations with the standard and modified version of Lund 7.3 compared to the experimental uncertainties.

6 Summary

Using the ARGUS detector we have analysed the inclusive production of the vector mesons $K^{*+}(892)$, $K^{*0}(892)$, $\rho^0(770)$ and, for the first time in e^+e^- annihilation, of the $\omega(783)$ meson in continuum events, direct $\Upsilon(1S)$ and $\Upsilon(4S)$ decays. Together with earlier ARGUS results we determined the vector meson and s quark suppression in direct $\Upsilon(1S)$ decays in a model independent way. V/(V+P) was found to depend on the quark content of mesons. The ratio (s/u) calculated from vector meson production agrees very well with (s/u) determined from baryon production. The results from continuum events agree with measurements at higher center of mass energies.
The Lund model cannot reproduce our measurements with default parameters, but it shows in general a good agreement to the data, if V/(V+P) and (s/u) are changed according to the results from direct $\Upsilon(1S)$ decays. Taking into account uncertainties due to charm branching ratios Lund 7.3 with modified parameters describes the measured inclusive multiplicities in the continuum as well as in direct $\Upsilon(1S)$ decays. Significant differences concern the shape of the z spectra for vector mesons from direct $\Upsilon(1S)$ decays. For continuum events discrepancies between data and simulation were found by comparing multiplicity ratios at different center of mass energies, where Lund predicts a smaller increase with $\sqrt{s}$ than measured. Comparisons

of continuum data to the model UCLA 7.31 give essentially the same discrepancies than mentioned for Lund 7.3.
A more detailed investigation of the fragmentation characteristics has to include also mesons from other multiplets than pseudoscalars and vectors. Because the massive resonances always decay to pseudoscalars but more seldom to vector mesons it is up to now impossible to deduce the relative production probabilities of vector and pseudoscalar mesons in fragmentation from the observable ratio V/(V+P). Unfortunately only very few measurements for the production of scalar or tensor mesons in fragmentation exist so far, so that new measurements on the production of heavier mesons are urgently needed.

Acknowledgements

It is a pleasure to thank U. Djuanda, E. Konrad, E. Michel, and W. Reinsch for their competent technical help in running the experiment and processing the data. We thank Dr. H. Nesemann, B. Sarau, and the DORIS group for the excellent operation of the storage ring DORIS II. The visiting groups wish to thank the DESY directorate for the support and kind hospitality extended to them.

References

[1] M. Derrick and S. Abachi, Part. Prod. in cont. e^+e^- Annih. at high energy (ed. P. Carruthers) (1988) 57, World Sci. Publ. Co.,
T. Hebbeker, Proc. of the Joint Int. Photon-Lepton Symp. (Geneva 1991) Vol. 2, 75.

[2] P. Söding and G. Wolf, Ann. Rev. of Nucl. Part. Sci. **31** (1981) 231.

[3] P. Abreu *et al.* (DELPHI), Phys. Lett. **B255** (1991) 466,
D. Decamp *et al.* (ALEPH), Phys. Lett. **B284** (1992) 151,
P. Abreu *et al.* (DELPHI), CERN-PPE-93-29 (1993), submitted to Z. Phys. C.

[4] R. Fulton *et al.* (CLEO), Phys. Lett. **B224** (1989) 455,
H. Albrecht *et al.* (ARGUS), Z. Phys. **C55** (1992) 25.

[5] A. Lindner, Doctoral thesis Dortmund (1992), *unpublished.*

[6] H. Albrecht *et al.* (ARGUS), Nucl. Instr. Meth. **A275** (1989) 1.

[7] Particle Data Group, Phys. Rev. **D45** (1992) 1.

[8] T.Sjöstrand, M. Bengtsson, Comp. Phys. Commun. **43** (1987) 367.

[9] J.D.Jackson, Il Nuovo Cimento **34** (1964) 1644.

[10] P. Abreu *et al.* (DELPHI), Phys. Lett. **B298** (1992) 236.

[11] P. D. Acton *et al.* (OPAL), Z. Phys. **C56** (1992) 521.

[12] O. Podobrin, DESY report DESY-FCE-92-03 (1992).

[13] *see e.g.* R. Brandelik *et al.* (TASSO), Phys. Lett. **B117** (1982) 135,
W. Bartel *et al.* (JADE), Phys. Lett. **B145** (1984) 441.

[14] R. J. Apsimon *et al.* (OMEGA), Z. Phys. **C53** (1992) 581.

[15] H. Albrecht *et al.* (ARGUS), Z. Phys. **C58** (1993) 199.

[16] H. Albrecht *et al.* (ARGUS), Z. Phys. **C46** (1990) 15.

[17] S. Behrends *et al.* (CLEO), Phys. Rev. **D31** (1985) 2161.

[18] H. Albrecht *et al.* (ARGUS), Z. Phys. **C41** (1989) 557.

[19] O. Behnke, Diploma thesis Hamburg (1992), *unpublished.*

[20] C. D. Buchanan, S. B. Chun, Phys. Rev. Lett. **59** (1987) 1997,
S. B. Chun, C. D. Buchanan, UCLA-HEP-92-008 (1992),
C. D. Buchanan, private communication.

[21] M.Aguilar-Benitez *et al.* (LEBC-EHS), Z. Phys. **C50** (1991) 405.

[22] H. Albrecht *et al.* (ARGUS), Z. Phys. **C44** (1989) 547.

[23] H. Albrecht *et al.* (ARGUS), Z. Phys. **C39** (1988) 177.

[24] H. Albrecht *et al.* (ARGUS), Z. Phys. **C43** (1989) 45,
H. Scheck (ARGUS), Phys. Lett **B224** (1989) 343,
H. Albrecht *et al.* (ARGUS), Z. Phys. **C49** (1991) 349.

[25] P. D. Acton *et al.* (OPAL), Phys. Lett. **B305** (1993) 407.

[26] N.M. Agababyan *et al.* (EHS-NA22), Z. Phys. **C46** (1990) 387.

[27] C.T. Jones *et al.* (WA21), Z. Phys. **C51** (1991) 11.

[28] G. Gustafson, C.Sjögren, Phys. Lett. **B248** (1990) 430.

[29] A. Breakstone *et al.* (ABCDHW), Phys. Lett. **B135** (1984) 510.

[30] H. Albrecht *et al.* (ARGUS), Phys. Lett. **B231** (1989) 208,
H. Albrecht *et al.* (ARGUS), Phys. Lett. **B232** (1989) 398.

[31] R. Mankel, private communication.

[32] H. Albrecht *et al.* (ARGUS), Phys. Lett. **B199** (1987) 291.

[33] W. Hofmann, Ann. Rev. Nucl. Part. Sci. **38** (1988) 279.

[34] P. Abreu *et al.* (DELPHI), Phys. Lett. **B275** (1992) 231.

[35] G. Alexander *et al.* (OPAL), Phys. Lett. **B264** (1991) 467.

[36] S. Abachi *et al.* (HRS), Phy. Lett. **B199** (1987) 151,
S. Abachi *et al.* (HRS), Phy. Rev. **D40** (1989) 706.

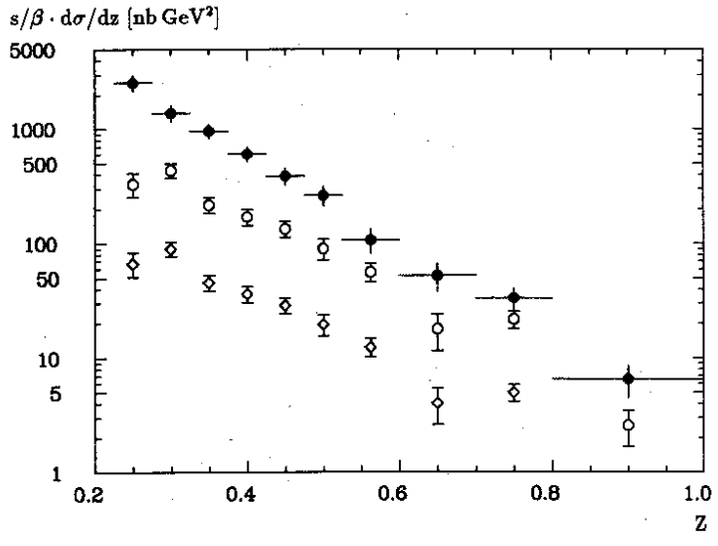

Figure 1: The K^{*+} spectra in $\Upsilon(1S)$ data (full dots), the scaled continuum (open dots) and the contribution from vacuum polarization (rhombs).

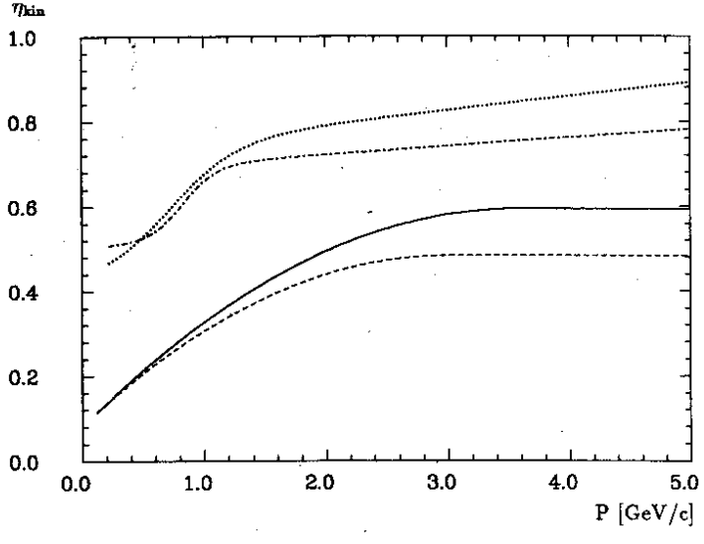

Figure 2: The model dependent part of the efficiency according to Lund 6.3 for K^{*+} mesons in continuum events (broken line) and direct $\Upsilon(1S)$ decays (full line) as well as for K^{*0} mesons (stroke-dotted and dotted resp.).

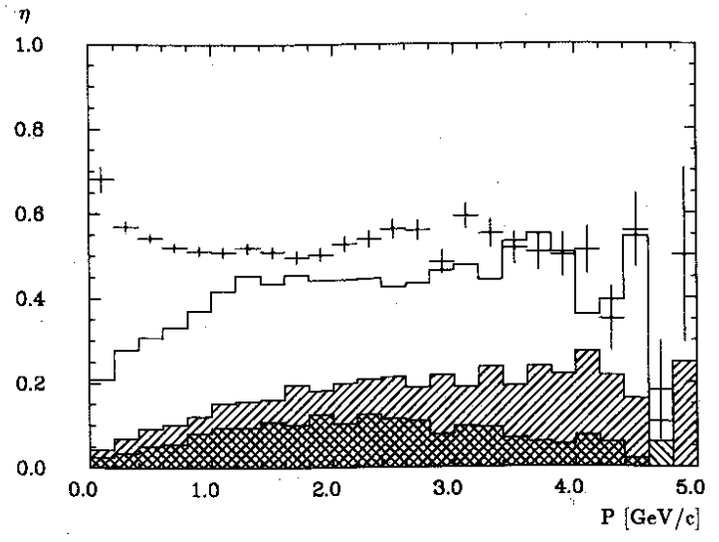

Figure 3: The efficiencies for ρ^0 (error bars), K^{*0} (histogram), K^{*+} mesons (hatched) and ω mesons (cross-hatched) in continuum events.

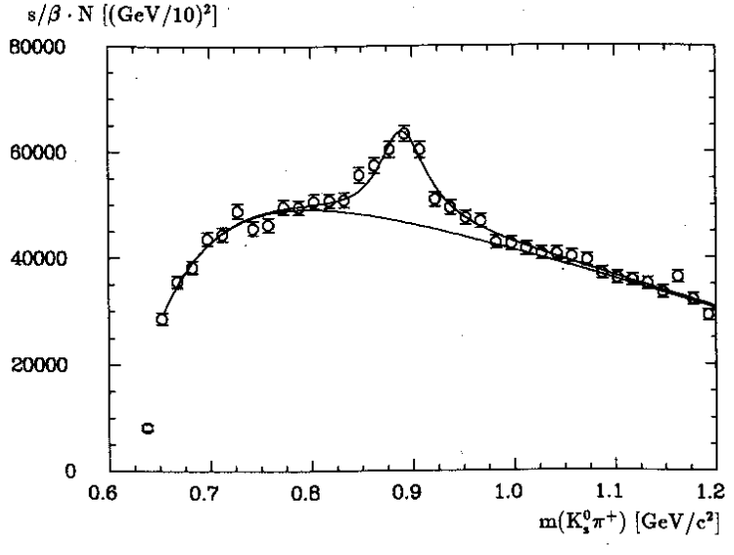

Figure 4: The K^{*+} signal ($z > 0.225$) on the $\Upsilon(1S)$ resonance with a fit to the data.

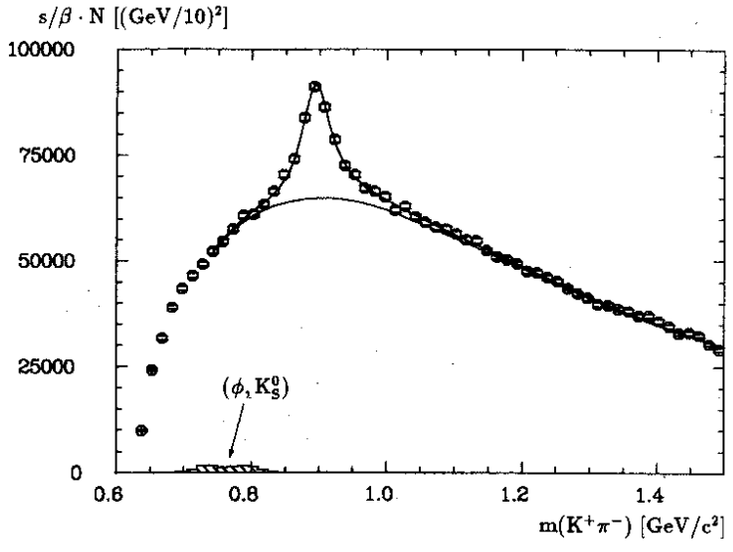

Figure 5: The K^{*0} signal ($z > 0.2$) on the $\Upsilon(1S)$ resonance with a fit to the data. The contribution from K^0_s and ϕ reflections is already subtracted (hatched histogram).

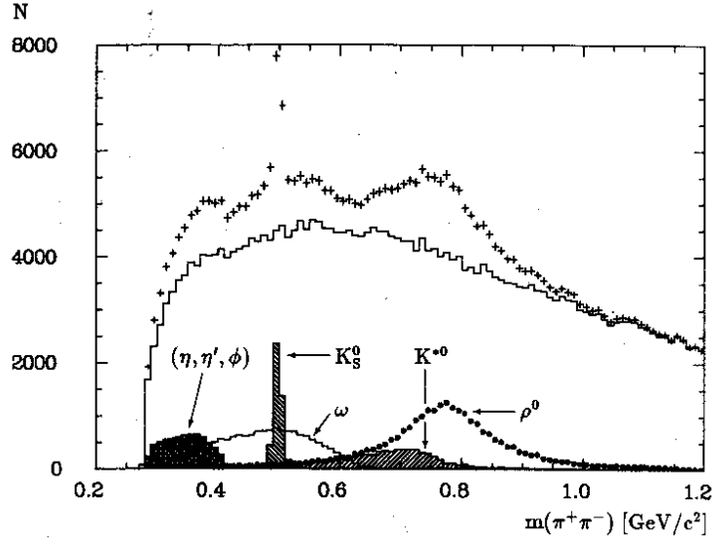

Figure 6: Contributions to the $\pi^+\pi^-$ mass spectrum according to the Lund model: The summed spectrum (crosses), the combinatorial background (line) and other components.

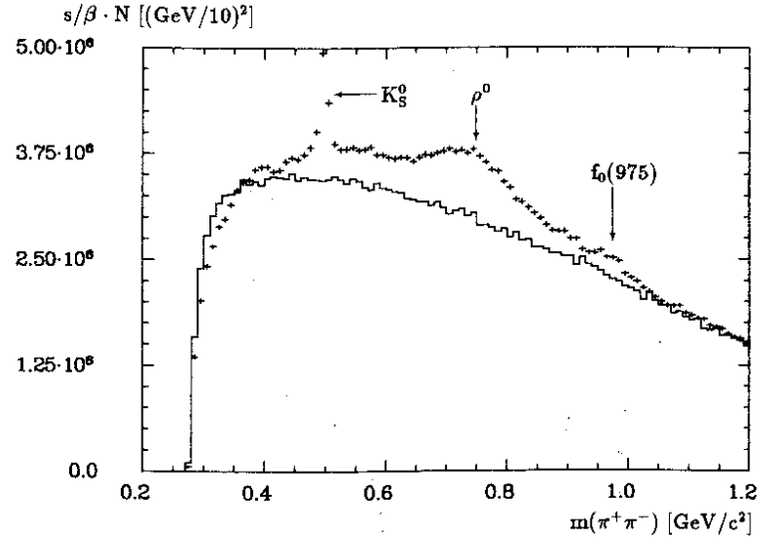

Figure 7: The invariant mass of $\pi^+\pi^-$ combinations (crosses) and weighted $\pi^\pm\pi^\pm$ combinations (histogram) on the $\Upsilon(1S)$ resonance (z>0.2).

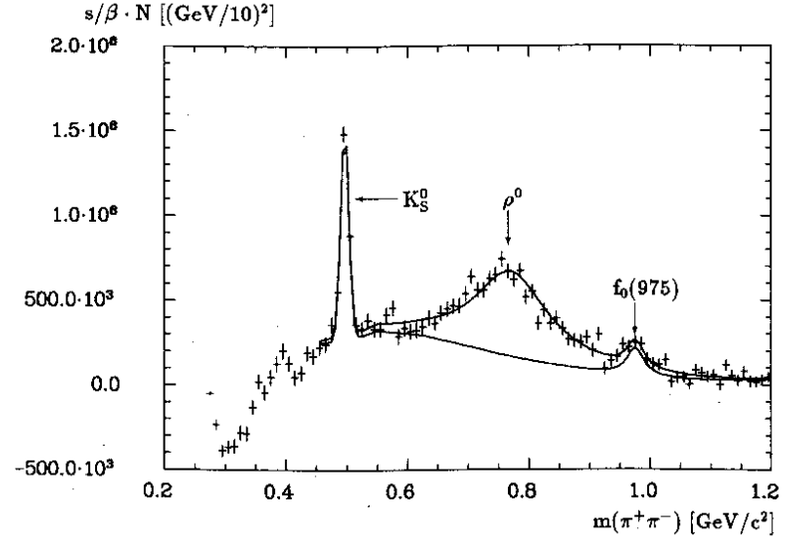

Figure 8: The ρ^0 signal ($z > 0.2$) on the $\Upsilon(1S)$ resonance with a fit to the data after subtraction of the K^{*0} reflection and $\pi^\pm\pi^\pm$ combinations.

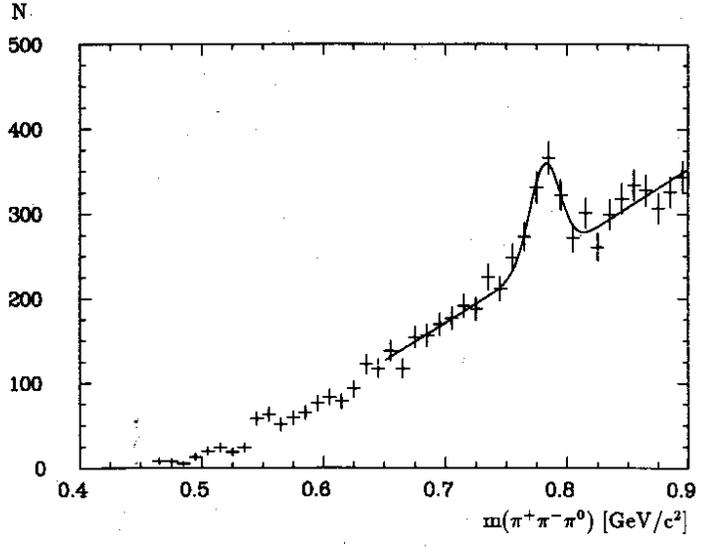

Figure 9: The ω signal (all data, p > 2 GeV/c) where converted photons were used to reconstruct π^0 mesons.

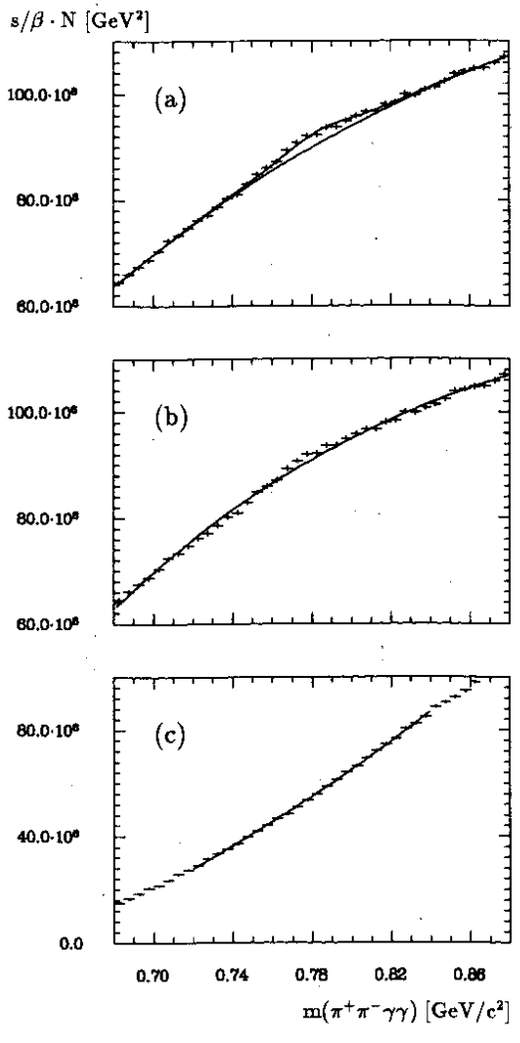

Figure 10: The ω signal on the $\Upsilon(4S)$ resonance ($0.2 < z < 0.85$): Part (a) shows the spectrum with a fit, while in (b) the ω contribution was fixed to zero. Figure (c) displays combinations, where only $\gamma\gamma$ combinations from a π^0 sideband were taken into account. No ω signal is visible.

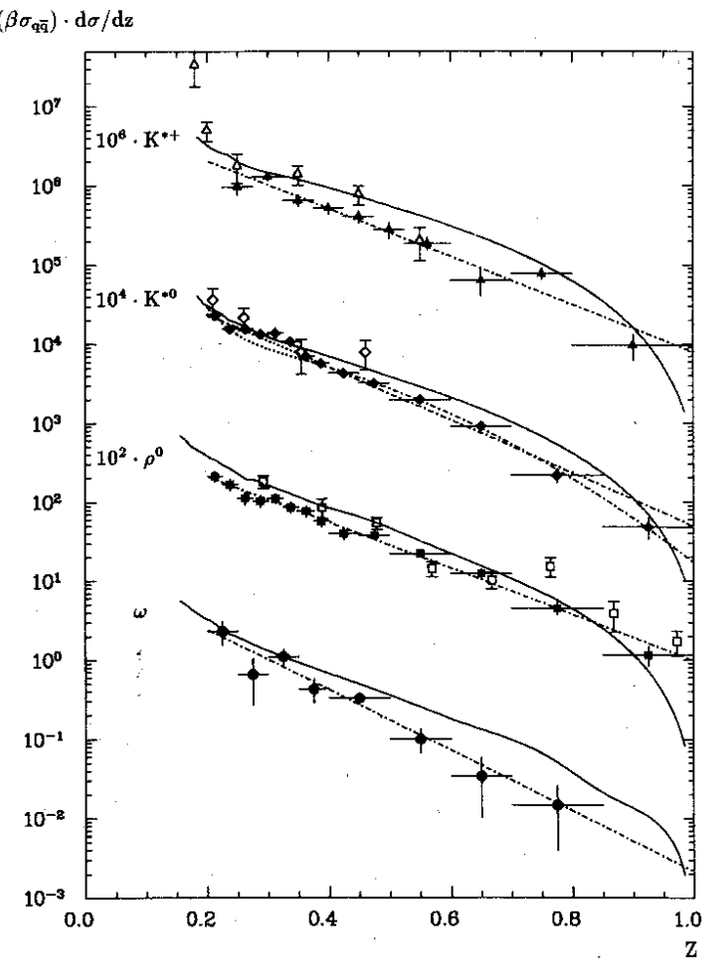

Figure 11: The vector meson spectra in continuum events as determined in this analysis (full dots) and by CLEO (open points). The dashed-dotted lines show the fits used for extrapolation, the full lines are predictions from Lund 7.3. Details are given in the text. Triangles display K^{*+} spectra multiplied by 10^6, rhombs K^{*0} spectra multiplied by 10^4, squares ρ^0 spectra multiplied by 10^2 and circles symbolize the ω spectrum.

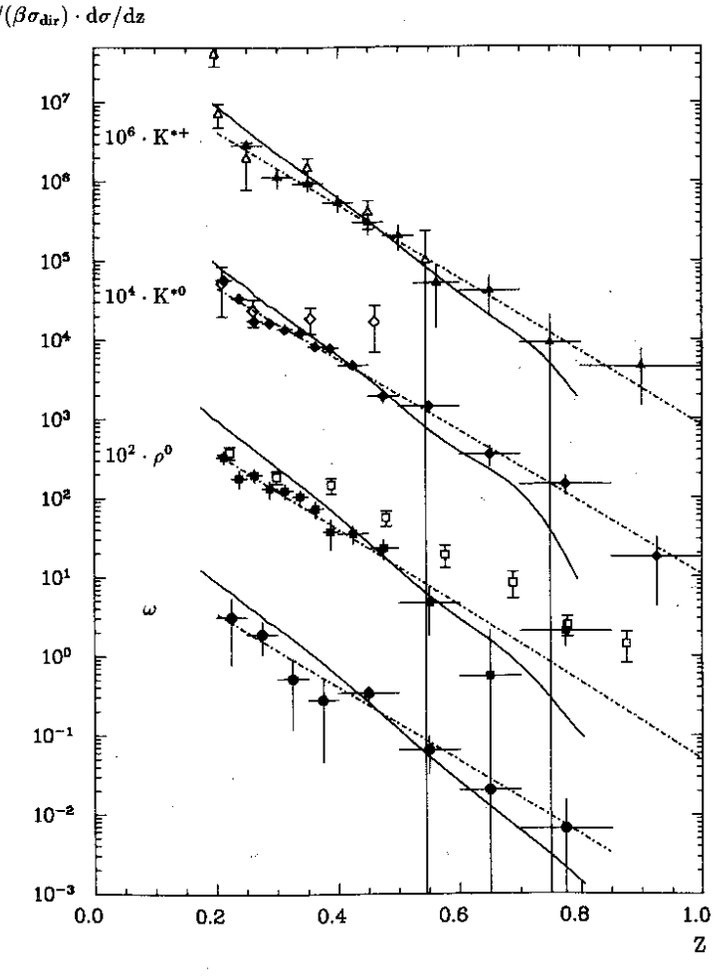

Figure 12: The vector meson spectra in direct $\Upsilon(1S)$ decays as measured in this analysis (full dots) and by CLEO (open points). The dashed-dotted lines show the fits used for extrapolation, full lines are predictions from Lund 7.3. Triangles display K^{*+} spectra multiplied by 10^6, rhombs K^{*0} spectra multiplied by 10^4, squares ρ^0 spectra multiplied by 10^2 and circles symbolize the ω spectrum.

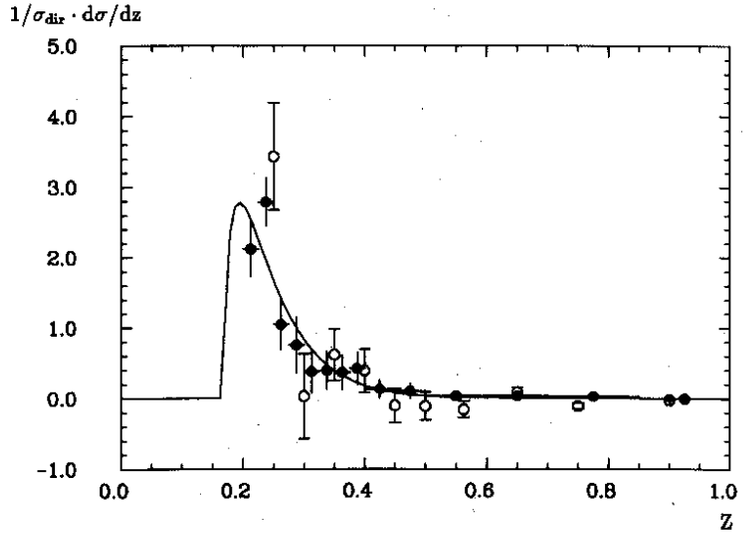

Figure 13: The K^{*0} spectrum (full dots), a fit used for extrapolation (line) and the K^{*+} spectrum (open circles) in $\Upsilon(4S)$ decays.

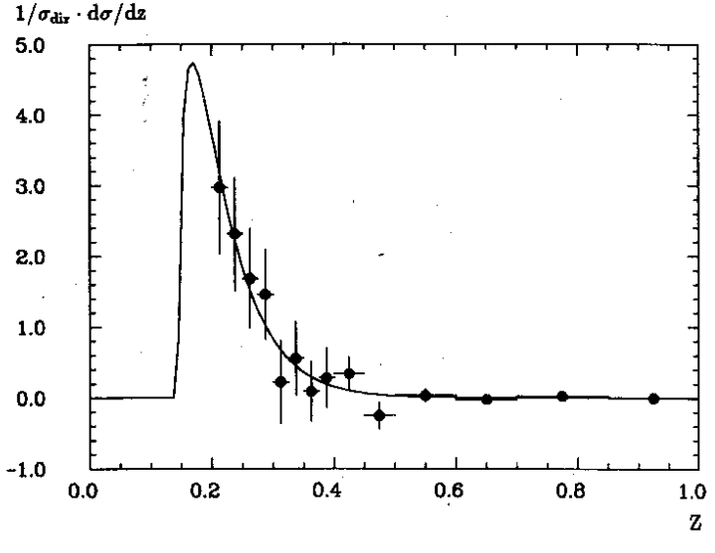

Figure 14: The ρ^0 spectrum in $\Upsilon(4S)$ decays and a fit used for extrapolation.

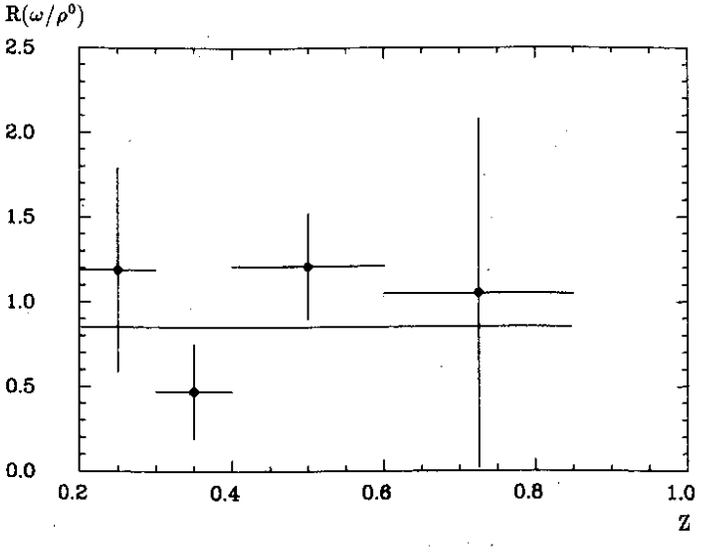

Figure 15: The ratio ω/ρ^0 of the spectra $1/\beta\sigma \cdot d\sigma/dz$ for mesons produced in direct $\Upsilon(1S)$ decays and a fitted constant.

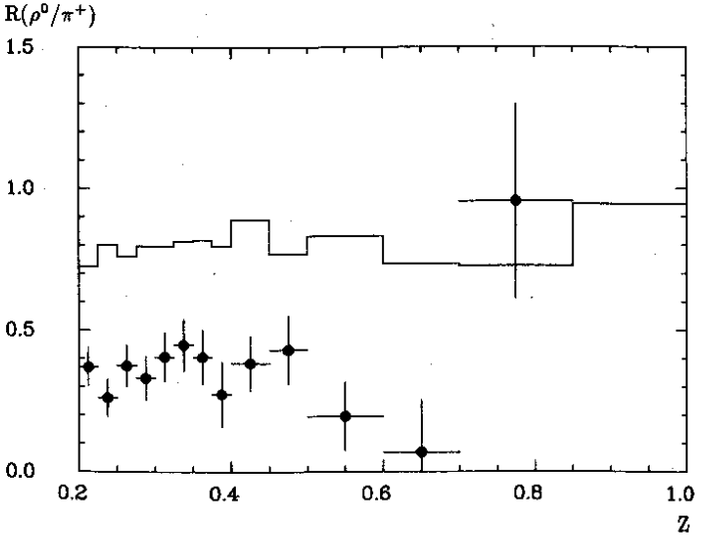

Figure 16: The ratio ρ^0/π^+ of the spectra $1/\beta\sigma \cdot d\sigma/dz$ for mesons from direct $\Upsilon(1S)$ decays from data (dots) and in Lund 7.3 (line).